NASA TECHNICAL NOTE

NASA TN D-5395

c. 1

NASA TN D-5395

SOLID-PROPELLANT COMBUSTION INSTABILITY AND THE ROLE OF VELOCITY COUPLING

by Louis A. Povinelli

Lewis Research Center
Cleveland, Ohio

NATIONAL AERONAUTICS AND SPACE ADMINISTRATION • WASHINGTON, D. C. • AUGUST 1969

NASA TN D-5395

SOLID-PROPELLANT COMBUSTION INSTABILITY AND THE ROLE OF VELOCITY COUPLING

By Louis A. Povinelli

Lewis Research Center
Cleveland, Ohio

NATIONAL AERONAUTICS AND SPACE ADMINISTRATION

For sale by the Clearinghouse for Federal Scientific and Technical Information
Springfield, Virginia 22151 – CFSTI price $3.00

ABSTRACT

This report is concerned with the role of pressure and velocity coupling in solid propellant combustion instability. The status of knowledge is reviewed, including current efforts directed toward improving propellant response theory. Recent work on driving mechanisms indicates the importance of velocity on the coupling process. The advantages and disadvantages of using the vortex burner and the T-burner for making response measurements are discussed. New results from the vortex burner are presented, regarding the effect of burning rate catalyst and aluminum oxide on the occurrence and severity of combustion instability. The relevance of the research results to rocket motors is discussed.

SOLID-PROPELLANT COMBUSTION INSTABILITY AND THE ROLE OF VELOCITY COUPLING

by Louis A. Povinelli
Lewis Research Center

SUMMARY

This report is concerned with the role of pressure and velocity coupling as contributors to the combustion instability phenomena in solid propellant burning. The current status of knowledge is reviewed starting with the linear theory of Bird, Hart, and McClure. Although this sophisticated theory is capable of predicting qualitative behavior of rocket motor stability it does not compare favorably with linear response measurements. Current efforts are directed toward improving the propellant response theory. Nonlinearities of the process are also being considered. Recent work on driving mechanisms have postulated the importance of velocity coupling. Experimental techniques are discussed, centering principally on the T-burner and vortex burner. The difficulty of using the end grain T-burner for the measurement of velocity coupled effects is discussed and the need for a new tool is described. Development of the vortex burner and the modified T-burner can fit the need. The distinction between the two burners is discussed. Previous results obtained with the vortex burner are reviewed and comparison is made with calculated response values. Some new information obtained in the vortex burner at Lewis Research Center is presented on the effects of burning rate catalyst (copper chromite) and an inert additive (aluminum oxide) on the occurrence and severity of instability. Limited information from a low frequency (800 cps) vortex burner is also presented. Comparison of the experimental results with response calculations, which are pressure and velocity sensitive, yields good agreement, thereby suggesting the importance of velocity effects.

The relevance of the research results to rocket motors is discussed. The immediate needs for further developments in instability research are presented within the context of providing useful design information.

INTRODUCTION

The design of solid-propellant rocket motors is complicated by the possible occurrence of combustion instability, especially in those situations where new grain configurations or propellant ingredients are employed. Various techniques for suppressing these chamber pressure oscillations have evolved, principally through trial and error techniques. In the past, the use of baffles or center rods has been effective in shifting acoustic cavity frequencies to higher modes which may be more difficult to drive or in preventing mean flow circulation associated with certain traveling modes. Consumable ignitor baskets to prevent pressure spiking caused by fragments passing through the nozzle and drilled holes through the propellant grain have been useful in some instances. These techniques have the disadvantage of incorporating additional components or propellant complexity in the motor design.

Hence, propellant modification has been exploited as a means for elimination of the combustion instability. These modifications have involved the judicious choice of metal additives of various size distributions as well as oxidizer type and size and propellant curing time. The fuel (or binder) has also been noted, in certain instances, to have a significant influence on the occurrence of combustion instability. The appropriate choice of propellant ingredients can also reduce the potential for agglomeration of metal additives (refs. 1 to 3), thereby yielding optimum oxide particles for viscous and thermal damping in the gas phase (ref. 4). It is noted that the addition of small amounts of fine aluminum powder has been one of the most successful techniques used to date in the suppression of the instability phenomena. However, there is no assurance that aluminum powder will be effective in future propellant combinations (ref. 5). This dictates the need for a more thorough understanding of the instability problem.

In the development of large-sized motors it is advantageous, and oft-times necessary, to perform small scale testing of propellant candidates prior to full-scale construction and firing. This reduced scale testing has been performed in (a) conventional rocket geometries with or without pulsing charges (refs. 6 to 8), (b) center-vented or T-burners, and (c) vortex or pancake burners (refs. 9 and 10). Although this testing yields some qualitative information regarding the relative stability of various propellant combinations, it cannot be carried over directly to the full sized motor because of scaling difficulties. These difficulties are associated with understanding and determining the individual gain and loss mechanisms in each particular motor geometry, be it subscale or full scale. Further research is required in separating the important driving and loss factors in the complex, viscoelastic, combusting, acoustically oscillating system.

Recent efforts to understand solid propellant combustion instability have indicated the importance of considering the effects of both pressure and velocity coupling mechanisms (refs. 9, 11, 12, and 13). This combined effect has been investigated in a vortex burner, and the experimental data support the postulated driving mechanism which arises from preferential energy addition in the presence of mean flow (ref. 14). This report reviews these previous results and presents new information on effects of additives in pressure and velocity coupled acoustic combustion instability. Additionally, the report reviews the status of knowledge in acoustic solid propellant combustion instability.

SYMBOLS

A	activation energy
A_s	activation energy associated with activated complex
$\mathscr{A}$	surface activation energy parameter
a	speed of sound
b	erosive exponent
C	burning rate constant
C_m	mass of particles/mass of gas in unit volume
$\mathscr{C}_1$	ratio of erosive to strand burning rate
E	erosive burning factor
f	frequency
g	gravitational constant
i	imaginary component of complex quantity
J	viscous dissipation term
$\mathscr{K}$	wall loss factor
k	erosive constant
k_1	Boltzmann constant
l	length of gas column in burner
M	Mach number
$\mathscr{M}$	burning rate parameter
m	propellant mass flux
m^*	mass rate rate of solid converter to gas resulting from successful collision
N	propellant response, $N = (w'/\overline{w})/(p'/\overline{p})$
n	steady state pressure exponent ($r = Cp^n$)
P	gas phase parameter

P_{rr}	stress tensor in solid grain
p	pressure
p_a	partial pressure of species a
R	particle radius
Re	real part of complex quantity
r	linear regression rate
Srr	stress displacement vector in solid
T_o	surface temperature of propellant
t	time
v	gas velocity
w	energy release rate or mass addition
Y	specific acoustic admittance of combustion zone
$Y(a)$	normal admittance of gas to solid at burning propellant surface
y	real part of specific acoustic admittance = $\rho g l (\alpha_g + \alpha_d)/2a^2 \rho_s r$
α	acoustic attenuation
α_c	exponential growth rate due to combustion
α_d	exponential decay rate constant
α_g	exponential growth rate constant
α_t	thermal diffusivity of solid
γ	specific heat ratio of combustion products
λ	complex frequency function
μ/ϵ	pressure coupled propellant response function = $Re(m'/\overline{m})/(p'/\overline{p})$
μ'	dynamic viscosity
ξ	amplitude factor
ρ	gas density
ρ_s	solid density
τ_d	particle relaxation time
ω	angular frequency

Subscripts:

a	species a

m mean value

s solid phase

Superscripts:

~ or ' denotes perturbed quantity

— denotes mean value

BACKGROUND AND REVIEW

Response Calculations

Numerous reviews have appeared in the literature on the subject of solid propellant combustion instability, the most recent ones being by Trubridge (ref. 15), Hart and McClure (ref. 16), and Price (refs. 17 and 18). These papers, give a fairly complete summary of the field of solid propellant combustion instability and cover the range from practical motor difficulties to the most elegant theoretical analysis. A review of work prior to this time is given in reference 19. A sophisticated theoretical treatment of a solid rocket system was that of Hart, McClure, and Bird (ref. 20), which is a linearized, one-dimensional thermal treatment of the solid-gas system. Gas phase reactions were assumed to occur over a very narrow zone giving rise to characteristic reaction times much smaller than the heat conduction and mass transport times. On this basis, only the heat conduction and mass transfer were considered as time dependent quantities. Their results were expressed in terms of an acoustic admittance Y, which is the ratio of the amplitude of the acoustic velocity normal to the surface of the acoustic pressure amplitude. In general the acoustic admittance is a complex quantity so that the velocity response to a pressure perturbation is described by a phase angle as well as a magnitude. The response function μ/ϵ is related to the admittance in the following way:

$$Y = -\frac{v}{p}\left(\frac{\mu}{\epsilon} - \frac{1}{\gamma}\right)$$

This response is a measure of the perturbation in mass flux normalized by the corresponding pressure perturbation:

$$\frac{\mu}{\epsilon} = \frac{\left(\frac{m'}{\overline{m}}\right)}{\left(\frac{p'}{\overline{p}}\right)}$$

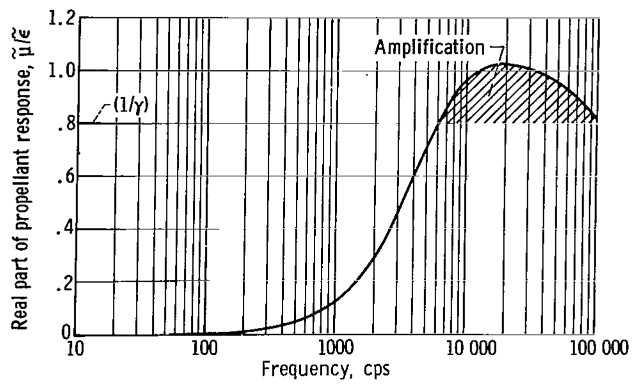

Figure 1. - Surface amplification as function of frequency for hypothetical propellant having zero state pressure exponent (from ref. 20).

The results of Hart, McClure, and Bird (ref. 20) shown in figure 1, indicated that the propellant surface was capable of amplifying an acoustic disturbance over a broad range of frequencies. As shown in figure 1, amplification occurs when the response exceeds the appropriate loss level (in this case, $1/\gamma$). In figure 2(a) the calculated acoustic gain and losses are plotted as a function of the fraction of web burned for a center perforated propellant grain. For any point in time, or distance burned, a balance between the visco-elastic loss, gas attenuation, and propellant amplification determined whether the motor is burning stably or unstably. The resulting map of the instabilities is shown in figure 2(b). The Hart-McClure criterion for stability therefore is given as:

$$\underbrace{\frac{-v}{\rho a^2}\left(\gamma \mathrm{Re}\,\frac{\mu}{\epsilon} - 1\right)}_{\substack{\text{Propellant}\\ \text{amplification}}} - \underbrace{\mathrm{Re}\left[Y(a)\right.}_{\substack{\text{Gas phase}\\ \text{attenuation}}} + \left.\underbrace{\frac{i\omega Srr}{-Prr}}_{\substack{\text{Solid}\\ \text{phase}\\ \text{atten-}\\ \text{uation}}}\right] < 0$$

which is a simple gain-loss balance concept. Evaluation of the individual terms, however, poses considerable problems. The viscoelastic behavior of the solid, the condition of propellant-to-case bonding, gas phase attenuation, and propellant erosivity were also considered; and it was demonstrated that by appropriate summation of the losses and gains the linear theroy could predict intermittent periods of instability during a rocket motor firing. This transition from stable to unstable burning was in qualitative agreement with experimental testing. The participation of the solid phase in the instability was demonstrated experimentally (ref. 21) as was the importance of propellant to case bonding (ref. 22).

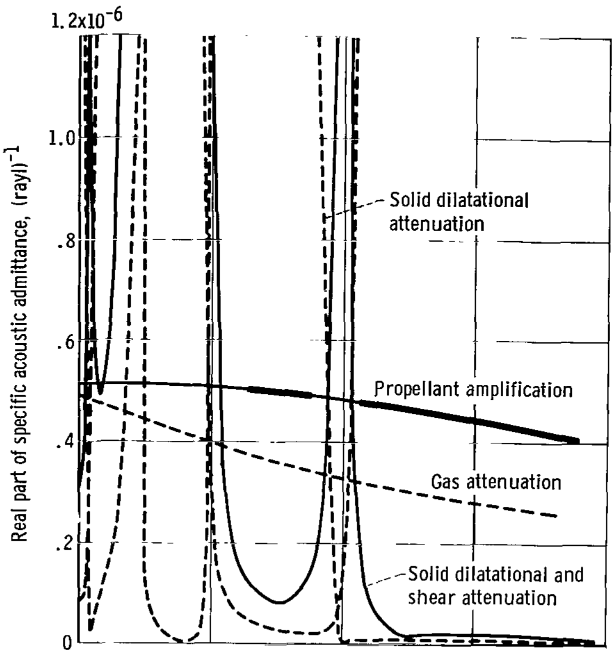

(a) Acoustic loss and gain balance along lowest second tangential gas quasi-mode of rocket motor, the grain being free to move at its outer boundary.

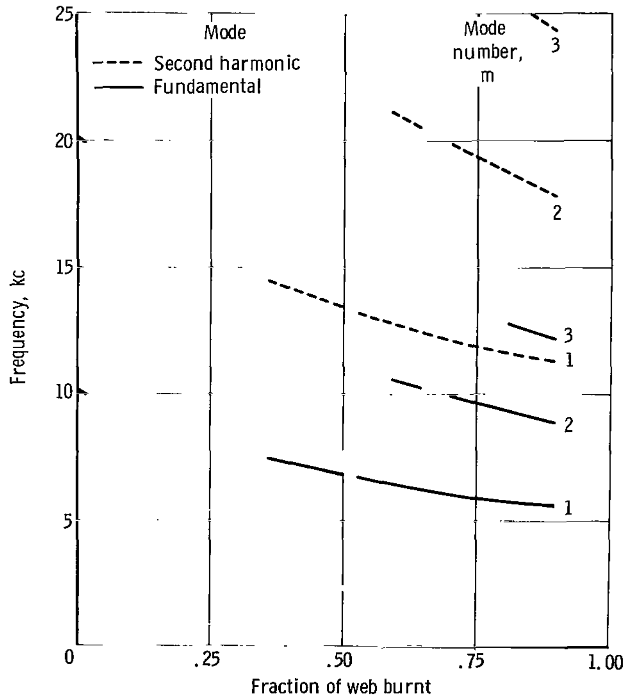

(b) Map of instabilities in radial and tangential modes of rocket motor, the grain being rigidly clamped at its outer boundary.

Figure 2. - Theoretical combustion stability behavior of center-perforated grain (from ref. 20).

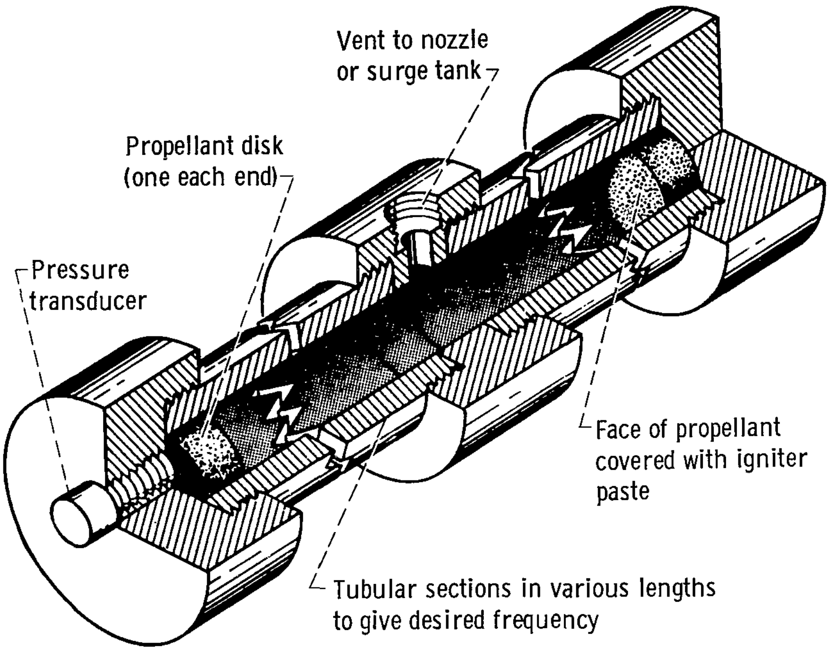

(a) Double-end burner for pressure-coupled instability.

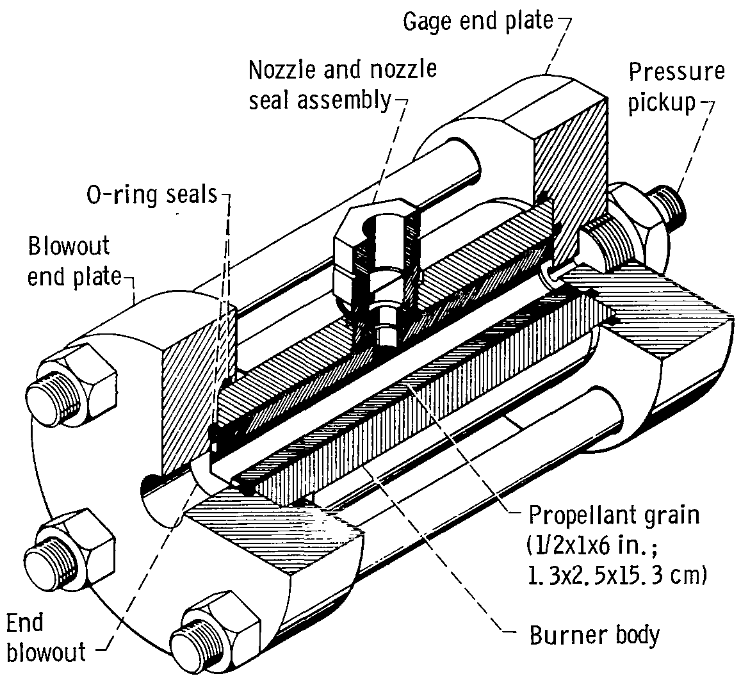

(b) Tubular burner exhibiting both pressure-coupled and velocity-coupled instability.

Figure 3. - Low-loss laboratory burners for study of oscillatory combustion. Burners exhaust through sonic nozzle or to constant-pressure surge tank (from ref. 17).

Since the dynamic aspects related to stability were characterized by the acoustic admittance, the T-burner was operated with end grains (fig. 3(a)) so as to provide a rigorous source of experimental data for comparison with the linear theory (ref. 23). During the growth and decay periods of the pressure oscillations in the T-burner the behavior is very nearly linear; hence these data may be used for the determination of an experimental admittance for comparison with the results of the linear theory. Figure 4

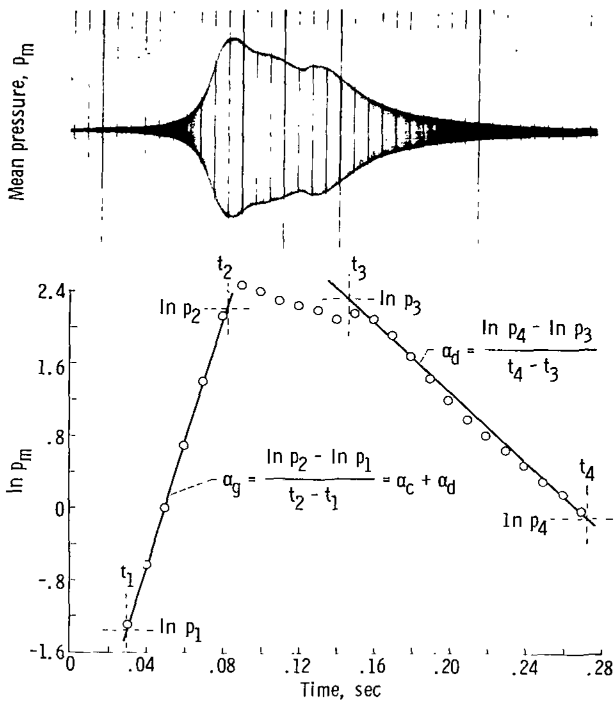

Figure 4. - Envelope of pressure oscillations and growth-decay rate calculations for T-burner in figure 3(a) (from ref. 64).

shows the envelopes of the pressure oscillations and a plot of the growth and decay periods. Whereas the oscillations grow exponentially, the decay is only approximately exponential and leads to some ambiguity in data reduction. If it is assumed that the length of the combustion gas column during the growth period is equal to the length of the combustion cavity, the response function is given by

$$\frac{\mu}{\epsilon} = \frac{p}{4a\rho_s r_s}\left(\frac{\alpha_g - \alpha_d}{f}\right)$$

or in terms of the admittance function as

$$Y = -\frac{l}{2\rho a^2}(\alpha_g - \alpha_d)$$

Figure 5 shows the comparison of the specific acoustic admittance between the experimental T-burner data for four pressures and the theoretical calculation. Agreement between theory and experiment was not encouraging either qualitatively or quantitatively (ref. 23).

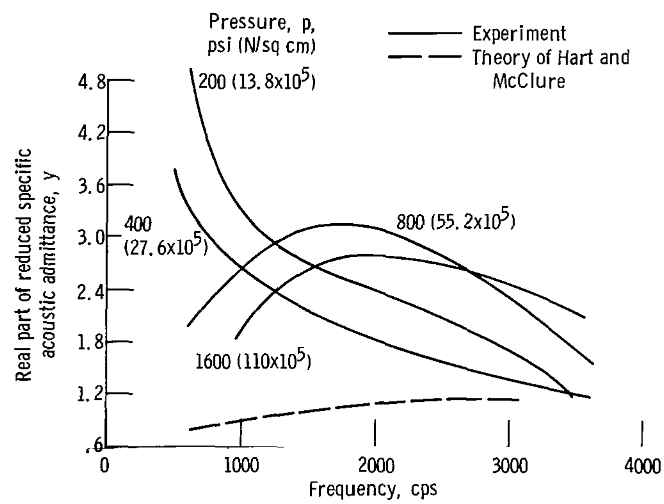

Figure 5. - The real part of reduced specific acoustic admittance as function of frequency for double-base propellant JPN (from ref. 23).

Consideration of additional factors in the linear theory, such as the effect of thermal radiation on the propellant response (ref. 24) met with only limited improvement. Some question also exists regarding the analysis of the T-burner itself which is required for the determination of the admittance function from the pressure measurements (ref. 25). The effects of the exit orifice, velocity and thermal boundary layers, and thermal radiation on the analysis of the T-burner were considered. The principal difficulties appear to be that the linear theory does not predict a sufficiently broad response or sufficiently large response to correspond to the linear experimental data. The contribution of velocity effects were considered in only a restrictive manner (ref. 26), namely, amplification could occur only if flow reversal took place giving rise to in phase energy addition.

Recent improvement in the linear theory was obtained by assuming that the gasification of a homogeneous propellant is essentially a thermally controlled decomposition described in terms of an Arrhenius law (ref. 27).

$$r = B(T_o)\exp\left(\frac{-A}{RT_o}\right)$$

Use of an autocatalytic regression rate expression, which allows for the possibility of surface reactions as well as the dependency of the surface reaction on pressure, has yielded good agreement between theoretical acoustic pressure response values and experimental data obtained with a double-base propellant (see fig. 6), although the activation energies used are considered too low (ref. 25). The autocatalytic model, which is written as

$$m = \frac{m^* P_a}{\sqrt{2\pi m_a k_1 T_o}} \exp\left(\frac{-A_s}{RT_o}\right)$$

assumes quasi-steady behavior in the gas phase and is applicable therefore only to those frequencies where the relaxation time is small relative to the time associated with the pressure disturbance.

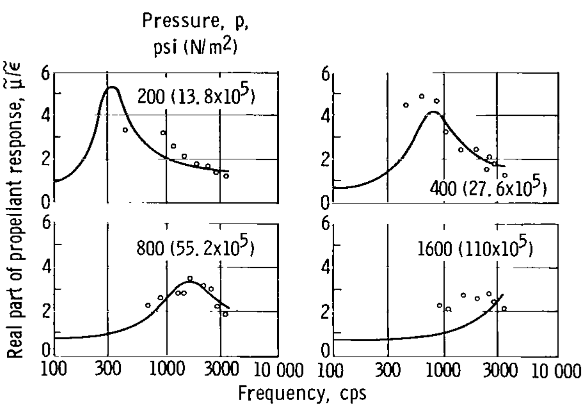

Figure 6. - Comparison of acoustic response calculated from model with experimental data of Horton and Price (from ref. 27).

Dennison and Baum considered a linear thermal theory with no surface reactions, a quasi-steady gas phase, and perturbed the conservation equations (ref. 28). The relaxation time associated with the gas phase processes again was considered short relative to the time associated with pressure oscillations. This quasi-steady treatment of the gas allows one to ignore time dependent terms. The analysis also considered the phase reactions between fuel and oxidizer vapors to be concentrated in a thin zone. The stability behavior was expressed in terms of two parameters; one being a sensitivity of the gas

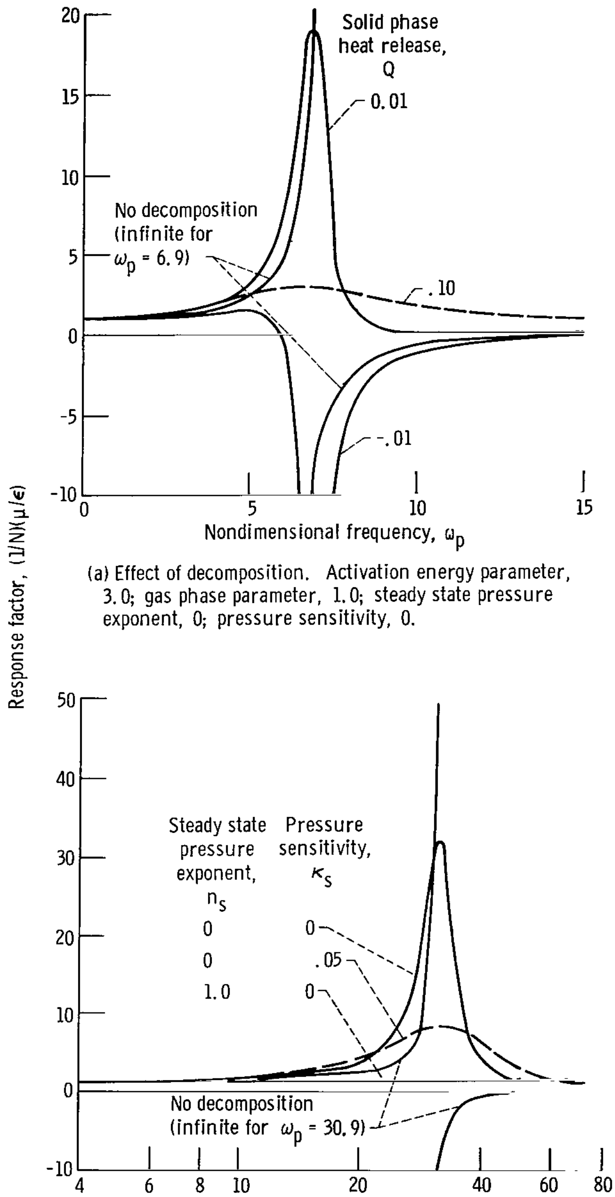

(a) Effect of decomposition. Activation energy parameter, 3.0; gas phase parameter, 1.0; steady state pressure exponent, 0; pressure sensitivity, 0.

(b) Effect of decomposition and surface reactions sensitive to pressure. Activation energy, 10.0; parameter, 6.0; solid phase heat release, 0.01.

Figure 7. - Theoretical response factors. Length of decomposition zone, 1.0; temperature sensitivity, 0.05 (from ref. 30).

phase to pressure fluctuations, the other being essentially the surface activation energy. The work of Dennison and Baum has been modified to include surface pyrolysis and surface-coupled exothermic or endothermic reactions which follow Arrhenius laws (ref. 29). The gas phase is treated as a premixed flame which also obeys Arrhenius kinetics. Culick (ref. 30) has additionally considered the presence of a pressure dependent decomposition zone at the solid surface. The presence of this zone was found to decrease the maximum response but did not alter the frequency at which it occurred. The decomposition zone, therefore, acted as a damping mechanism. As shown in figure 7(a), very large maxima (infinite values in some cases) are found in the limit of no decomposition. The peaks are reduced and smoothed when decomposition is included. The variables considered include a solid phase heat release Q, a parameter related to the surface activation energy $\mathscr{A}$ and a gas phase pressure sensitive parameter P. Also included are the thickness l, temperature sensitivity δ_s, pressure sensitivity κ_s of the decomposition zone, and n_s, which is the pressure sensitivity of the surface region. Among the results calculated in reference 30, it is shown in figure 7(b) that increasing the pressure sensitivity of the decomposition zone (κ) or the surface (n_s) leads to a significant decrease in the propellant response. One of the difficulties associated with the analysis is the prediction of a negative response function (ref. 31). The inclusion of surface coupled exothermic or endothermic reactions within a kinetics framework that is more general than the one-step description used by Culick (ref. 30) and a more realistic gas phase description appears to circumvent this difficulty (ref. 31). The results also show that a very small change in the surface-coupled heat release may have a profound effect on the amplitude of the pressure coupled response. Calculations for a typical composite propellant show that the peak response is doubled when there is 10 percent of the total heat release at the surface. Figure 8 shows a broadening of the response function as the solid (A) and gas (P) phase kinetics parameters are increased. For single step surface kinetics, surface-coupled exothermic reactions also yield a damping influence on the amplitude of the steady oscillatory response, as found by Culick (ref. 30).

The contribution of pressure-sensitive interfacial reactions to the acoustic admittance has also been studied (ref. 32). These interfacial reactions refer to the behavior between oxidizer crystals and the binder during regression. Coating the oxidizer crystals with substances known to be less reactive with the oxidizer than is the binder revealed a 50 percent reduction in the maximum experimental propellant response as shown in figure 9. Frequency shifts were found to occur for the maximum response position. Inclusion of the oxidizer coating material as an ingredient in the binder did not affect these pressure response measurements. It was postulated therefore that the contribution of interfacial reactions to the overall combustion process is reduced by the coating, which in turn reduces the admittance. Friedly and Peterson (ref. 33) have also considered the presence of exothermic reactions at the propellant surface. It can be shown (ref. 25) that

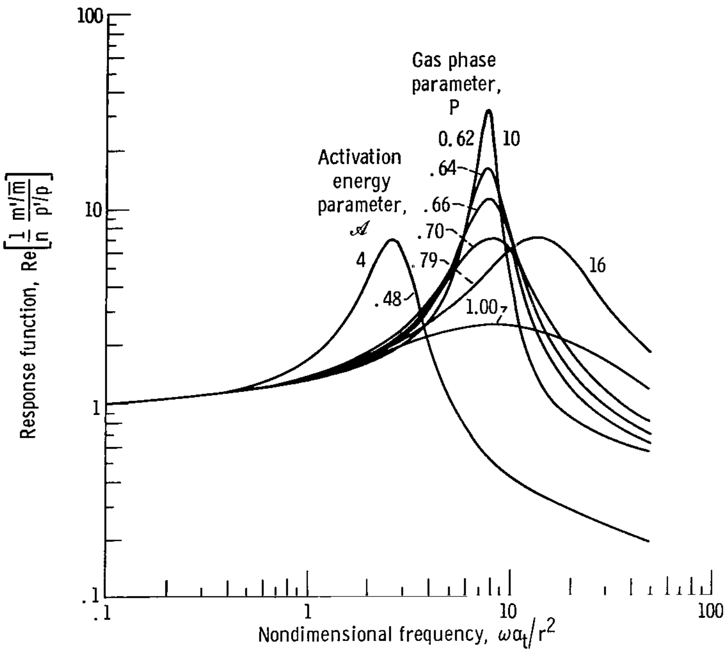

Figure 8. - Response function in oscillatory mode (from ref. 31).

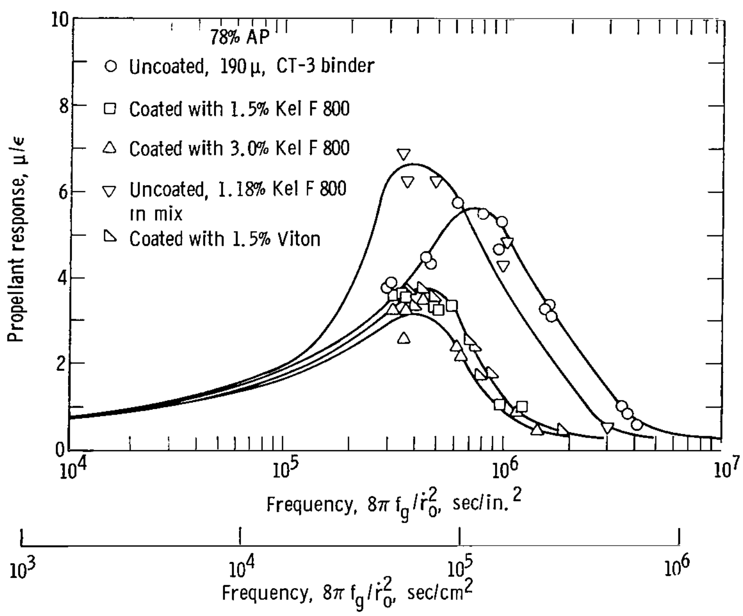

Figure 9. - Effect of Kel-F and Viton coatings on acoustical response (from ref. 32).

virtually all of these analyses discussed can be reduced to the Dennison-Baum form involving two principle parameters, namely,

$$\frac{\mu}{\epsilon} = \frac{\frac{m'}{\overline{m}}}{\frac{p'}{\overline{p}}} = \frac{nAP}{\lambda + \frac{A}{\lambda} - (1 + A) + AP}$$

for the case of no decomposition zone. A essentially represents the surface activation energy and P is the gas phase sensitivity to pressure disturbances.

Comparison of the theoretical response data with experimental measurements is now being pursued with both small volume nonacoustic (L^*) burner measurements for the lower frequency range and T-burner results for the higher frequencies with overlap of the measurements at the peak (refs. 34 and 35). It appears that the qualitative behavior of the calculated response function is sufficiently sensitive to the various effects (such as inclusion of surface reactions, presence of a decomposition zone, pressure dependency) so that the difference might be distinguished in experimental results (ref. 25). However, comparison of theory and data at high frequencies has not generally yielded good agreement (ref. 36, see fig. 10). The best agreement appears to be that obtained with am-

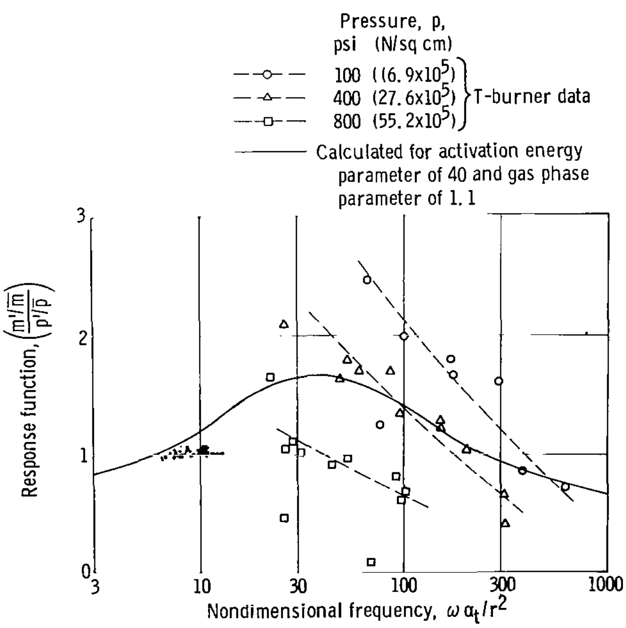

Figure 10. - The real part of the response function as function of nondimensional frequency for A-13 propellant (from ref. 36).

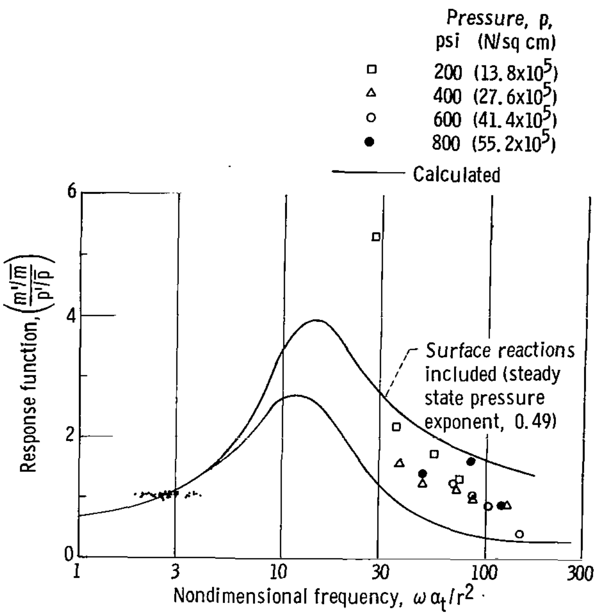

Figure 11. - Real part of response function as function of nondimensional frequency for A-35 propellant. Activation energy parameter, 14; gas phase parameter, 0.8 (from ref. 36).

monium perchlorate-polyurethane propellant as shown in figure 11. Low frequency results appear to be fairly well described by the Dennison-Baum theory.

It is noted that significant variations in the magnitude of the pressure response as measured in T-burners are obtained from various laboratories (ref. 37). Current efforts by the ICRPG Working Group on Solid Propellant Combustion are being made to resolve these differences in response measurements.

Some recent work has attempted to describe the gas phase flame zone in a more realistic fashion (ref. 38) by replacing the usual laminar premixed flame assumption and avoiding the postulate of isentropic behavior of the burnt gas at the edge of the flame zone. The concept of quasi-steady gas phase behavior is discussed and its usage interpreted relative to previous work. This modification, however, does not appear capable of reconciling the discrepancy between theory and experiment. It is worthwhile to note that theoretical response calculations, in general, fail to consider the heterogeneous nature of the composite propellant. One exception to this is the recent work by Williams (ref. 39) where a response function is formulated analytically in terms of the oscillation frequency and the frequency of heterogeneity. It appears as if a still more realistic description of the flame zone structure is required (ref. 40). In this report it is informative to review the diagnostic experiments that have been performed on the combustion region.

Flame Zone Structure

The presence of CN radiation has been used as an indicator of the reaction zone structure, based on the knowledge that this particular species could be formed only from a chemical reaction between the binder and oxidizer (refs. 41 and 42). The CN radiation in some premixed flames has been shown to be limited to the reaction zone with possible weak extensions into the burned gases. By combining the spectral emission of the propellants and a mercury light source (as shown in fig. 12) which served as a tracking device, the reaction zone thickness, the position of onset of CN radiation, and the position of maximum CN radiation were determined. The reaction zone at 1 atmosphere was found to have a thickness of 2000 micrometers and hence is not confined to a zone of

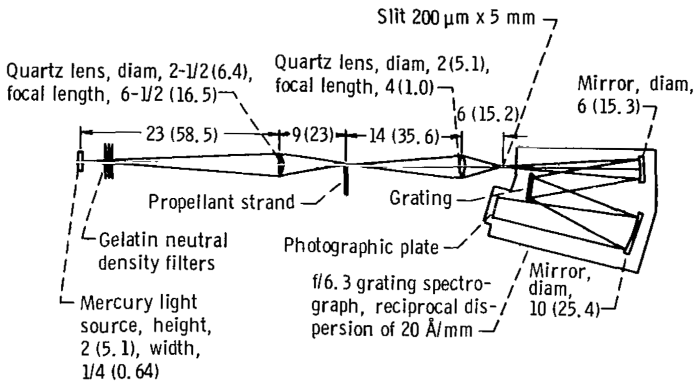

(a) Schematic of optical system.

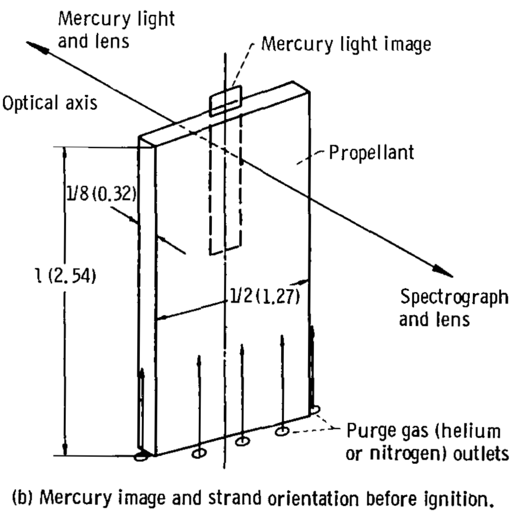

(b) Mercury image and strand orientation before ignition.

Figure 12. - Optical system for obtaining spatial resolution of flame gas species (from ref. 42). (Dimensions in inches (cm).)

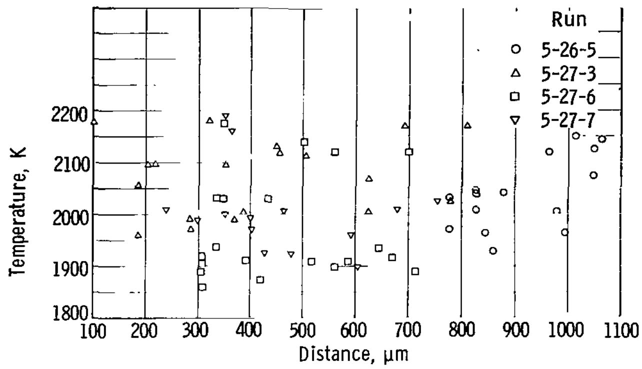

Figure 13. - Flame temperature of fine oxidizer grind propellant (6 μm AP, PS) (from ref. 44). Pressure, 215 pounds per square inch absolute (14.8×10^5 N/sq cm).

negligible dimension as assumed in most of the response analyses. Measurements over the pressure range of 1 to 20 atmospheres indicated a thickness of 200 to 1000 micrometers (ref. 43). Temperature measurements of the gas phase have also been made. In reference 44 a servosystem was employed to maintain the burning propellant surface at a fixed position, and the gas phase temperature was measured optically using the sodium D-line reversal technique. The results indicated that at a fixed position above the propellant surface the temperature varied from the lower limit of accurate temperature measurement, 1800 K, to the adiabatic flame temperature of the propellant, 2200 K, shown in figure 13. The size of the temperature measuring zone was 60 by 40 micrometers with a propellant thickness (optical path length) of 1000 micrometers. The fluctuations in gas temperature, from 1800 to 2200 K at distances of 100 to 800 micrometers above the propellant surface, occurred over the pressure range of 115 to 215 pounds per square inch absolute (7.9 to 14.8×10^5 N/sq m). It was concluded that the fluctuations in temperature were indicative of continuous reaction occurring over an 800 micrometer zone. Also it was shown that temperature profiles obtained with thermocouples embedded in the propellant could lead to profiles which were not unique (ref. 44). The work of Penzias (ref. 45) also shows wide variations in the gas phase temperature.

The interpretation given these results is that the reaction zone is of the order of 1000 micrometers in thickness with continuous reaction occurring between fuel and oxidizer components. The behavior is not that of a premixed gas flame but rather a diffusion or mixing limited flame. Hence, although the relaxation time associated with the local gas phase burning is short relative to the wave time, the diffusion or mixing of the fuel-oxidizer vapors may not be so. Hence the mixing time can introduce a significant time delay and must be considered as a time dependent quantity in the feedback loop. The existence of a thick reaction zone therefore has a profound influence on the form of the analytical equations used for determining the propellant response. Inclusion of this more realistic description of the flame zone may yield a satisfactory fit of the available experimental data. Whether the thick reaction zone concept will cause a shift of the response curve to different frequencies and yield a larger maximum value remains to be evaluated.

The optical temperature measurements of reference 44 indicate that values close to the adiabatic flame temperature occur within 100 micrometers of the burning propellant surface. The spectrographic observations in reference 41 show the onset of the reaction zone occurs at about 70 micrometers above the surface. The results of Sutherlands' measurements (ref. 46) showed that the active reaction zone occupies only 100 micrometers or less adjacent to the propellant surface. Penzias, however, obtained values close to 800 micrometers before adiabatic flame temperature is reached. It is noted that all of these measurements suffer inaccuracies either due to optical limitations or nonuniqueness (due to spatial variations as discussed in ref. 44) of the thermocouple measurements. However, one may estimate the energy flux from the propellant gases back to the solid propellant surface for a range of temperature gradient values, assuming a one-dimensional temperature profile. Following the calculations of Friedman (ref. 47) wherein a flux of 200 calories per gram (8.4×10^5 J/g) is required for vaporization of the solid and a solid density of 2 grams per cubic centimeter, a conductivity of 0.0002 calorie per centimeter-second-^{o}C (0.84 J/(cm)(sec)(^{o}C)), a burning rate of 1 centimeter per second, and a 2000^{o} C temperature gradient, a value of 10 micrometers is obtained for the gradient distance. If one assumes a distance of even 100 micrometers, it can be shown that only 10 percent of the energy flux (relative to 200 cal/g, 8.4×10^5 J/g) required is incident at the propellant surface (see fig. 14). This indicates that additional heat sources are required to sustain the deflagration. The most evident source is the exothermic reaction involved in ammonium perchlorate decomposition. Estimates of the energy flux from AP decomposition, based on thermocouple measurements and a heat balance (ref. 48), run approximately 130 calories per gram (5.5×10^5 J/g). The possibility of surface reactions between oxidizer and binder constituents at or below the surface has also been postulated

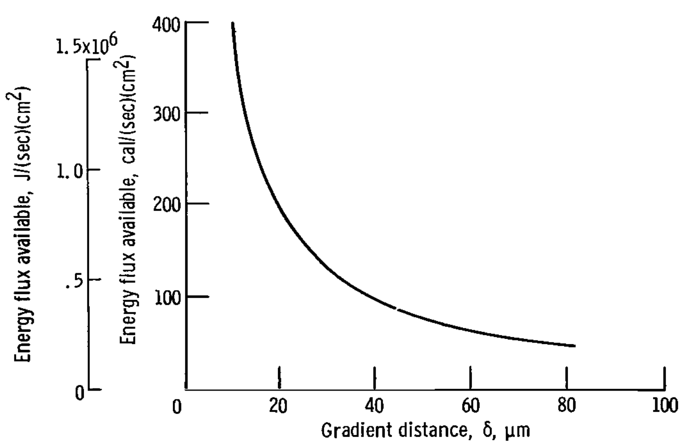

Figure 14. - Energy flux to burning surface (from ref. 40).

as an additional energy source (ref. 49). However, no direct experimental evidence exists to justify the presence of condensed phase reactions. Extinguished samples of oxidizer-binder sandwiches show no hint of interfacial reactions (refs. 50 and 51). Hence it is concluded that energy flux from the burning propellant gases and the result of the exothermic decomposition of ammonium perchlorate and endothermic fuel polymer decomposition provide all the energy required for sustaining the burning of the propellant. It appears, therefore, that in order to accurately represent the combustion behavior in analytical terms, the energy terms should contain both a surface component due to exothermic oxidizer decomposition and a gas phase conductive term, such as in reference 30. The inclusion of a term arising from subsurface reactions of fuel and oxidizer constituents does not appear to be justified.

Inclusion of the concept of a thick reaction zone and the presence of energy sources in the gas and at the solid phase are considered to be critical requirements in the analytical formulation of the acoustic response of composite solid propellants containing ammonium perchlorate. The extensive or thick zone implies that the premixed treatment is invalid. Hence, realistic mixing or a diffusion zone is required. In regard to the solid propellant surface certain microscopic irregularities associated with the realities of its decomposition behavior may also need to be considered. These further requirements include the presence of a liquid sublayer (ref. 52), and thermal stress cracking of crystals. The effects of oxidizer size and quantity, three-dimensional effects, and other nonhomogenities must also be considered. Hopefully, reasonable agreement between theoretical pressure response and one-dimensional experimental data will be achievable without a complete accounting of all the complexity of the decomposing surface structure. Indeed, the details of a deflagrating surface of a composite propellant, particularly those containing metal additives, must be a cause of considerable dismay for the conscientious theoretician.

Nonlinear Effects

In addition to the difficulty regarding proper flame structure modeling, several other factors require consideration, namely, nonlinear effects, velocity coupling, and relaxation of the quasi-steady assumption for the gas flow. Relatively little work has been performed on the nonlinear analysis of solid rocket instability. References 38 and 53 present an extension of the linear analysis to the nonlinear calculation of the response factor. The theoretical results are found to be critically dependent on the assumptions made as to the structure of the flame zone during dynamic perturbation. In this situation, a large amplitude velocity disturbance parallel to the surface sweeps away agglomerated metal particles. Subsequent velocity oscillations sweep off finer particles with a shorter combustion time. These finer particles have a combustion delay which is consistent with the requirement for velocity-coupled instability. Response values determined by the linear analysis agree quite well with the nonlinear values at low amplitude disturbances but show lower values for amplitudes of 20 percent or higher (ref. 38). Larger amplitudes were also found to increase the phase difference between the pressure and burning rate.

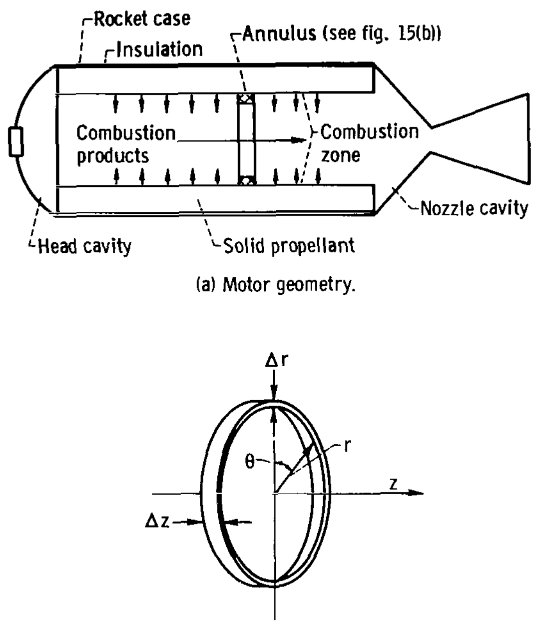

(a) Motor geometry.

(b) Annular element.

Figure 15. - Geometry of analytical model (from ref. 54).

Another analysis which includes solid rocket motor losses and gains is presented in reference 54 and employs a numerical perturbation technique. The analytical geometry is shown in figure 15. Both pressure and velocity response are included, through the use of an empirical burning rate expression which does not include the details of the flame zone. The grain was assumed to decompose and react in accordance with the normal strand rate expression with an additive erosive effect. Quasi-steady behavior was assumed with no variation in the propellant response with frequency. The resulting form of the energy equation was

$$\rho' \frac{\partial T'}{\partial t'} = -\rho\left(v'_\theta \frac{\partial T'}{\partial \theta'} + v_z \frac{\partial T'}{\partial z'}\right) + Jf(j)\frac{\partial^2 T'}{(\partial\theta')^2} - |\gamma - 1|p'\left(\frac{\partial v'_\theta}{\partial\theta'} + \frac{\partial v'_z}{\partial z'}\right)$$

$$+ \frac{4}{3}|\gamma(\gamma - 1)|J\left[\left(\frac{\partial v'_\theta}{\partial\theta'}\right)^2 + \left(\frac{\partial v'_z}{\partial z'}\right)^2 - \frac{\partial v'_\theta}{\partial\theta'}\frac{\partial v'_z}{\partial z'}\right]f(\gamma)$$

$$+ \mathscr{M}\omega'\left[\gamma - T' + \frac{(\gamma - 1)}{2}\gamma\left(v_z'^2 + v_\theta'^2\right)\right] - (P' - 1)^2$$

The structure of the acoustic mode and the mean flow is taken into consideration. The pressure-time behavior is used as an indicator of motor stability; the pertinent parameters arising from the nondimensionalization of the conservation equations being pulse size ($\Delta P/P$), a burning rate parameter $\mathscr{M} = \rho_s r_s/\rho_0 a$, a viscous dissipation term J, and a wall loss factor $\mathscr{K}$. The results as shown in figure 16 indicate the regions of stable and unstable operation obtained from observing the amplitude of the pressure oscillation with time. The effect of introducing erosive burning E of varying degree changes the pressure stability boundary by a large amount as seen in figure 17. An increase in the pressure exponent (fig. 18), a decrease in the port Mach number (fig. 19) and an increase in the erosive burning all tend to reduce the region of stable operation. Verification of these theoretical results with motor data remains a challenge.

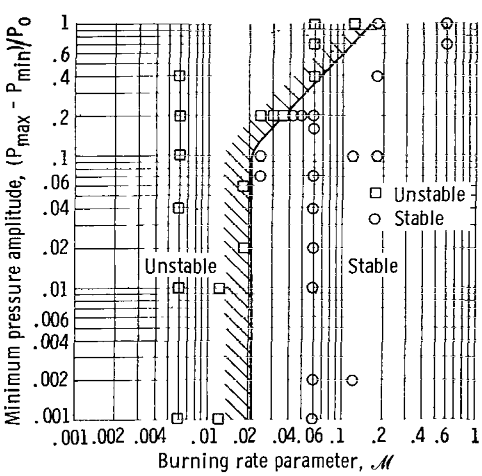

Figure 16. - Combustion stability limits for pressure response only. Pressure exponent, 0.4; erosive burning factor, 0; axial Mach number, 0.01; viscous dissipation parameter, 3×10^{-11}; wall-loss parameter, 0.003 (from ref. 54).

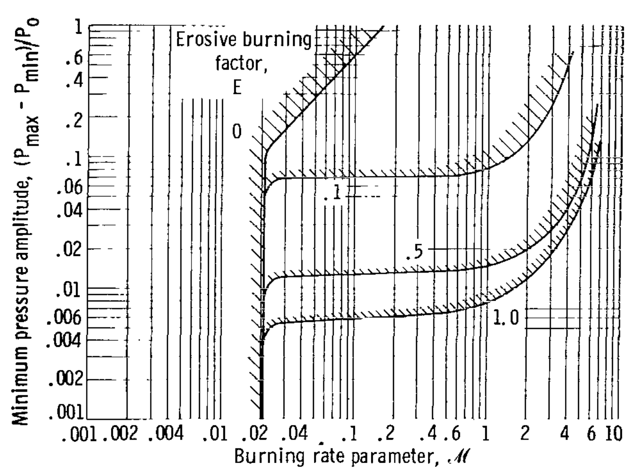

Figure 17. - Erosive burning effect on combustion stability limits. Pressure exponent, 0.4; erosive exponent, 0.8; axial Mach number, 0.01. Unstable region is above and to the left of stability boundaries (from ref. 54).

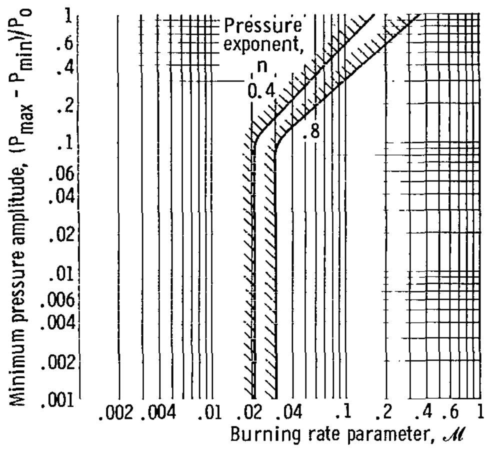

Figure 18. - Effect of pressure exponent on combustion stability limits. Axial Mach number, 0.01; erosive burning factor, 0. Unstable region is above and to the left of stability boundaries (from ref. 54).

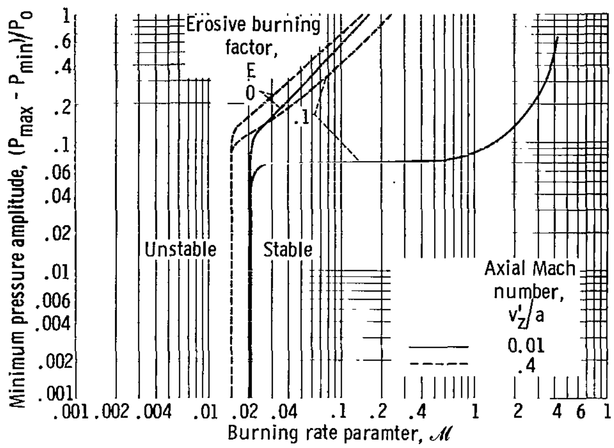

Figure 19. - Axial velocity effect on combustion stability limits. Pressure exponent, 0.4; erosive exponent, 0.8. Unstable region is above and to left of stability boundaries (from ref. 54).

Velocity Coupling

The contributions of velocity effects have been considered in the situation where flow reversal could give rise to the occurrence of in-phase energy addition (ref. 26). As shown in figure 20, if a longitudinal mode possesses sufficient amplitude, regions of flow reversal may occur at the head end of a rocket motor. Since the combustion response is sensitive to the magnitude of velocity, unequal effects are produced during each half cycle and amplification may occur. The effect is a nonlinear one due to rectification of the velocity during flow reversal. It is known, however, that amplification due to velocity coupling can occur in the presence of mean flow without reversal; provided propellant erosivity occurs. Theoretical analysis of velocity coupling has proceeded either employing a threshold erosivity (i.e., no erosion below a threshold velocity) or a mean flow effect leading to in-phase energy addition. In the case of threshold erosivity the combustion

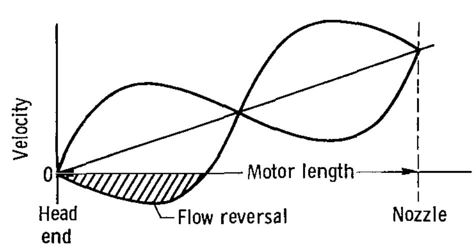

Figure 20. - Head end flow reversal in presence of high amplitude oscillation (from ref. 59).

rate is assumed to depend on velocity only after a threshold velocity v_0 is exceeded. In reference 11 it was assumed that an axial standing mode existed in a cavity and the local acoustic velocity V_0 was additive to mean flow velocity $\bar{v}$. An arbitrary time lag between the combustion response and the pressure perturbation was assumed. Figure 21 illustrates the manner in which driving of the acoustic disturbance may arise for three situations, namely, threshold velocity greater than, equal to, or less than the mean velocity V, where $V = \bar{v} + V_0$. It may be seen in figure 21 that as the sum of the local acoustic and mean velocities exceeds the threshold velocity v_0, a combustion response occurs which may lead to in-phase energy addition. The amplification at any given point in the motor depends on the local structure of the acoustic field, the mean flow velocity, and the amplitude of the oscillation. (The second and third portions of the combustion response in fig. 21(c) appear to be inconsistent with figs. 21(a) and (b) where the regions of no com-

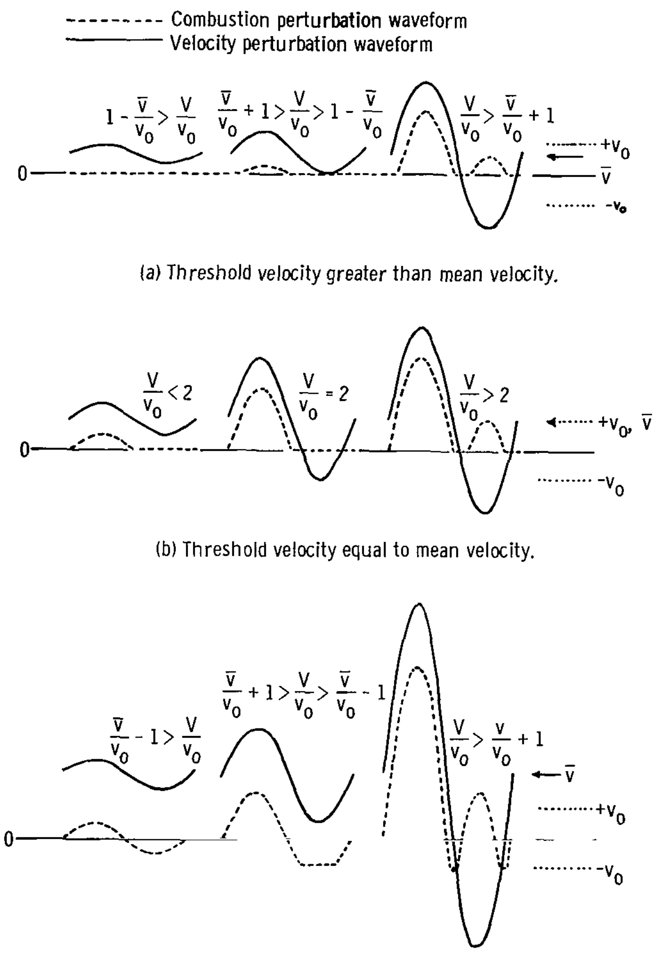

(c) Threshold velocity less than mean velocity.

Figure 21. - Waveform of combustion perturbations for various combinations of mean velocity, threshold velocity, and velocity amplitude (from ref. 11).

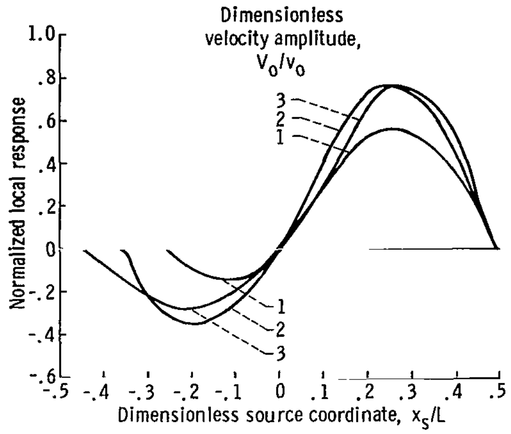

Figure 22. - Variation of first mode pressure response with axial location. Velocity distribution, linear; relative time lag, one-quarter cycle; geometrical factor, 1; response factor, ratio of maximum mean to threshold velocity, 1.

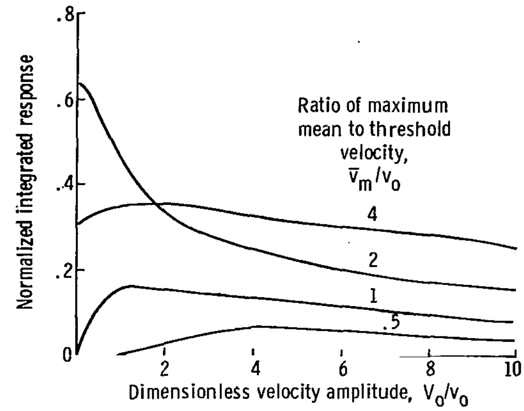

Figure 23. - Integrated first mode propellant response as function of amplitude of first mode oscillation. Velocity distribution, linear; relative time lag, one-quarter cycle; geometrical factor, 1; response factor, constant (from ref. 11).

bustion response correspond to the zero velocity line. These two responses should be raised by the magnitude v_o.) The local velocity response for the assumed axial mode was determined as a function of spatial location along the motor length. Figure 22 shows the contribution of a dimensionless channel length element X_s/L to the acoustic mode amplification during one cycle of oscillation. It is noted that the two ends of the motor, for the three values of the acoustic to threshold velocity amplitudes shown, produce opposing effects on amplification. This situation however is dependent on the time lag between acoustic oscillations and combustion oscillation and may become additive if the lag decreases toward the nozzle end. Summing up the contributions to amplification over the entire motor leads to a single number which is a function of the ratio of the acoustic velocity amplitude to the threshold velocity V_o/v_o and the ratio of the maximum mean velocity to threshold velocity $\bar{v}_m/v_o$ (see fig. 23). These results were obtained assuming a fixed time lag between the combustion and acoustic oscillations and a linear growth of velocity along the grain. Pressure-coupled contributions are not included in the analysis, nor are the losses. The results suggest the futility in attempting to explain instability trends in terms of one-dimensional combustion models without regard for the structure of the acoustic and mean flow field (ref. 11).

Some experimental work has indicated that aluminum particles contained in the solid propellants may also play an important role in velocity coupling (ref. 55). In this situation, a large amplitude velocity disturbance parallel to the surface sweeps away agglomerated metal particles. Subsequent velocity oscillations sweep off finer particles with a shorter combustion time. These finer particles have a combustion delay which is consistent with the requirement for velocity-coupled instability.

The approach followed at Lewis Research Center (ref. 14) and at Sheffield University (ref. 56) is now discussed within the framework of this report.

DRIVING MECHANISM AND CALCULATIONS

As mentioned previously, driving may arise out of the nonlinear effects due to rectification of the velocity during flow reversal. As shown in figure 24, however, it is not necessary to have flow reversal in order to obtain velocity-coupled wave amplification. With no steady flow the response is proportional to the magnitude of the velocity oscillation irrespective of its direction. The combustion response is symmetrical over each half cycle and hence no driving occurs. However, with a steady flow the response is asymmetrical leading to more energy addition during alternate half cycles of the oscillations and hence amplification of the acoustic disturbance (ref. 14).

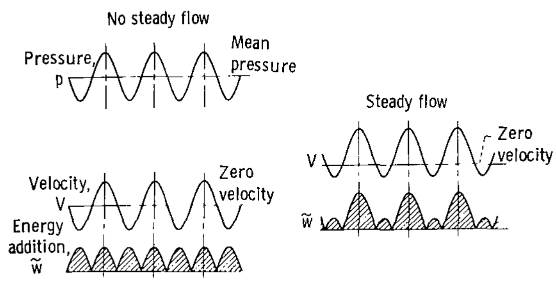

Figure 24. - In-phase energy addition due to mean velocity (from ref. 14).

The propellant burning rate was assumed to behave in a quasi-steady fashion (which introduces frequency limitations) in accordance with the following expression:

$$r = Cp^n + k(\rho v)^b$$

Normalizing the expression by $C\bar{p}^n$ and substituting for $p/\bar{p}$, $\rho/\bar{\rho}$, and $\bar{v}_\theta/a$ from the first order solutions of Maslen and Moore (ref. 57), for the first traveling acoustic mode results in the following expression for the normalized energy release which is assumed to be proportional to the instantaneous energy release:

$$\frac{w}{C\bar{p}^n} = (1 - 0.698\ \xi \cos t)^n + \mathscr{C}_1(1 - 0.582\ \xi \cos t)^b\left(\frac{\bar{v}_\theta}{a} + 0.0316\ \xi \cos t\right)^b$$

Assignment of values for the amplitude factor ξ, the pressure exponent n, the parameter

$$\mathscr{C}_1 = \frac{k(\bar{\rho}a)^b}{C\bar{p}^n}$$

the erosive exponent b, and the tangential Mach number $\bar{v}_\theta/a$ allows one to evaluate the amount of energy release. The oscillating energy release component in phase with the pressure was evaluated numerically over one cycle of oscillation in accordance with the expression

$$\tilde{w} = \int_{-\pi/2}^{\pi/2} (w - \bar{w})dt + \int_{\pi/2}^{3\pi/2} (\bar{w} - w)dt$$

where the average energy release $\bar{w}$ is evaluated as the integral of w dt over a cycle of oscillation. The ratio of $\tilde{w}/\bar{w}$ to $\tilde{p}/\bar{p}$ is then used as a measure of the real part of the propellant response to the imposed pressure and velocity disturbances. Typical results are shown in figures 25 and 26 for a $b = 0.6$, $n = 0.4$ with $\mathscr{C}_1$ as a variable, and $\Delta p/p = 7$ and 49 percent, respectively. Knowledge of the losses associated with the nozzle, solid phase material, head end cavity, and particulate matter enables one to predict the velocity range over which instability may occur (see fig. 26). Instability results when the response is greater than the loss level.

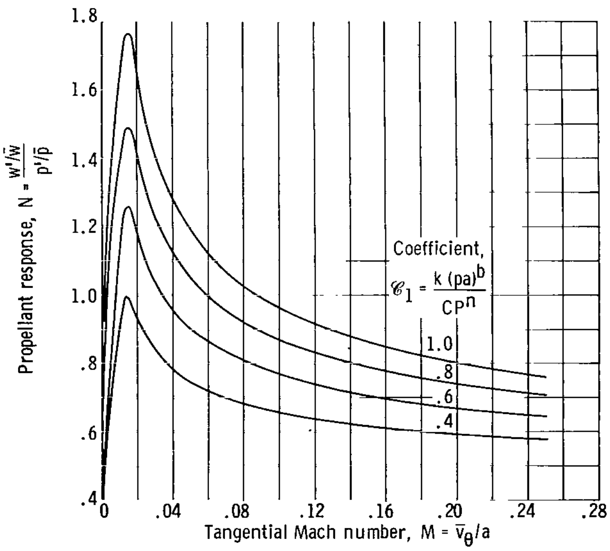

Figure 25. - Calculated response variation with Mach number. Peak-to-peak pressure amplitude, 7 percent (from ref. 14).

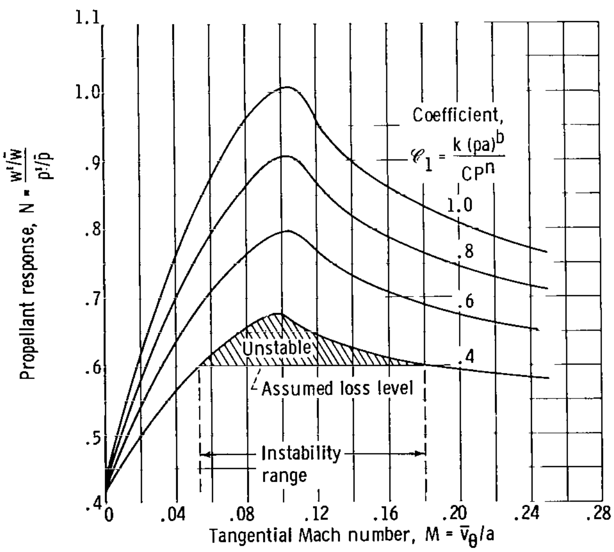

Figure 26. - Calculated response variation with Mach number. Peak-to-peak pressure amplitude, 49 percent (from ref. 14).

EXPERIMENTAL TECHNIQUES

Vortex Configuration

Development of the vortex or pancake combustor allows one to experimentally measure combined pressure and velocity coupling effects. This type of burner has L/D values less than unity. This experimental burner consists of three components: a main chamber, an instability jet, and a gas generator, as shown in figure 27 (ref. 14). The mode of operation involved the tangential injection of hot propellant gas from the generator into the main chamber, which had a center perforated grain. The injected gas causes both a mean vortex flow and a traveling acoustic mode to be established within the main chamber. Wave amplification occurs through pressure and velocity coupling. Motors of two sizes were used. The first was a 7-inch (17.8-cm) inside diameter main chamber with a 1/2 inch (1.27 cm) depth; the second being 24 inches (61.0 cm) in inside diameter by 1/2 inch (1.27 cm) deep. Whereas one generator was used for driving the instability in

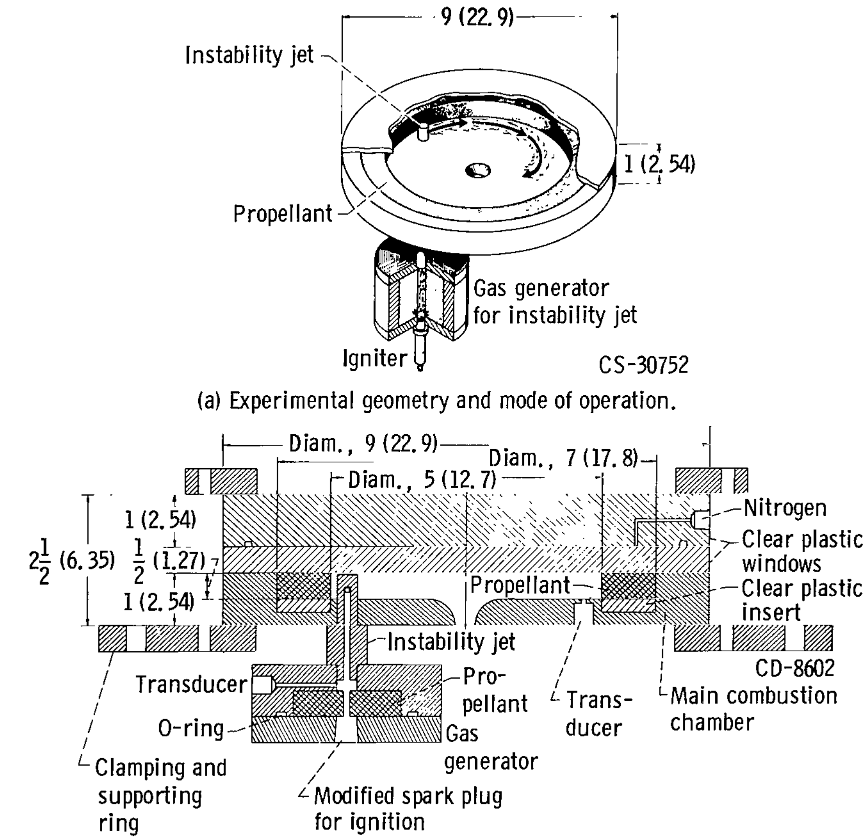

(a) Experimental geometry and mode of operation.

(b) Motor, gas generator, and instability jet assembly.

Figure 27. - Experimental combustor (from ref. 14). (Dimensions in inches (cm).)

the smaller size motor, two generators were coupled with the 24-inch (61.0-cm) chamber. These were positioned 180° apart and both injected burnt gases in the clockwise or counterclockwise direction. Only a limited number of tests (four) were run with the larger geometry.

Distinction Between Vortex and T-Burners

Since the T-burner has found wide appeal among research people, it is desirable to compare these research tools. The basic difference between the vortex and the normal end grain T-burner is illustrated in figure 28. In the vortex geometry a mean velocity exists over the surface of the propellant. As indicated, a point on the propellant surface experiences an in-phase pressure and velocity oscillation as the acoustic wave propagates around the cavity. In reality a portion of the burning propellant (rather than a point on) experiences the acoustic disturbance at any given time since the propellant is finite in width. The vortex burner has usually been operated with a steadily increasing mean velocity upon which is superimposed an oscillating component. In this fashion instability boundaries may be detected. In the case of the T-burner, a mean velocity does not exist at the propellant surface. The entire propellant surface experiences a pressure oscillation as indicated in figure 28. Steady gas flow occurs away from the propellant surface.

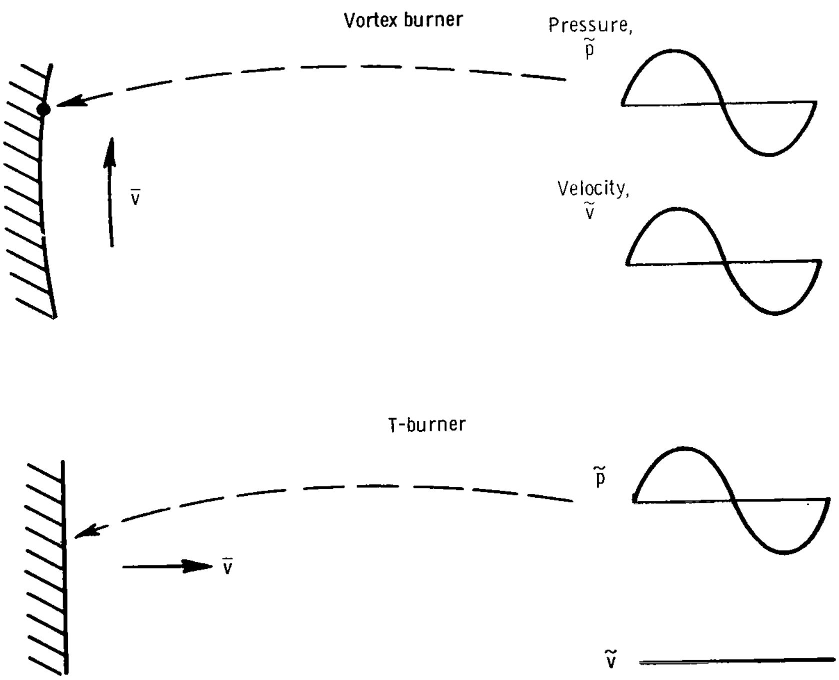

Figure 28. - Comparison of vortex and T-burner behavior.

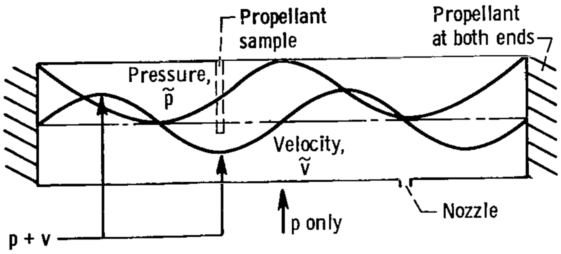

Figure 29. - Modified T-burner.

The principal difference between the vortex and T-burners is, therefore, that the vortex burner incorporates a high velocity flow over the burning propellant surface (thereby simulating rocket port conditions) whereas the normal T-burner does not include this effect. The T-burner configuration is unable, consequently, to include any effects that velocity coupling may have in combustion instability. Variations in the T-burner such as using tubular propellant charges as in figure 3(b) allow for velocity coupling but relative pressure-velocity phasing makes the results difficult to analyze. The modified T-burner, as shown in figure 29, makes use of small propellant samples located along the length of the burner at a position where both pressure and velocity oscillations occur. Results from this type of burner reveal significant contributions from velocity coupling (ref. 12). A disadvantage of this type of burner, however, is the distortion of the acoustic field caused by the propellant sample.

RESULTS AND DISCUSSION

General Behavior of Vortex Burner

The general pressure-time behavior is illustrated in figure 30. The increase of burning area within the gas generator yielded a gradually increasing pressure. The corresponding change in the main chamber pressure follows the generator output. In this manner it is possible to ramp through a pressure range and detect the instability boundary. The flow field within the motor was primarily tangential relative to the burning propellant surface and gradually increased in magnitude for about 6 seconds after which the generator ceased burning. The maximum pressure developed in the motor with the 1/2-inch (1.27-cm) throat was approximately 285 pounds per square inch absolute (1.96×10^6 N/sq cm). In the absence of tangential flow, the maximum operating pressure was experimentally observed to be 35 pounds per square inch absolute (24.5×10^4 N/sq cm). For the motor with a 3/4-inch (1.91-cm) throat the maximum pressure was 105 pounds per square inch absolute (72.4×10^4 N/sq cm). These large increases in motor chamber pressure were caused by addition of mass from the gas generator, erosive burning due to the high

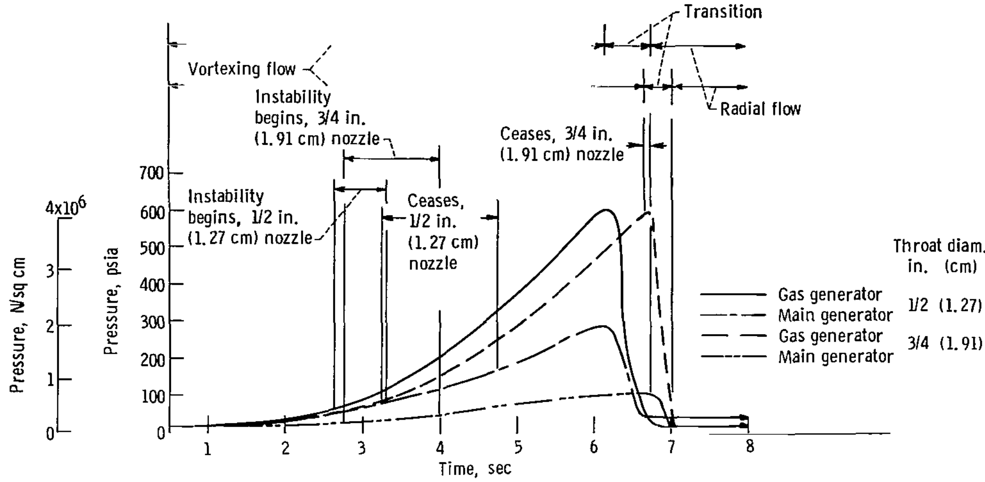

Figure 30. - Pressure-time behavior of gas generator and main chamber of vortex burner.

tangential velocities in the main chamber, and reduction of the effective nozzle throat area due to vortexing flow in the vicinity of the nozzle. The latter has been shown to be primarily responsible for the large chamber pressure (ref. 14). Since the increase in chamber pressure is accompanied by an increase in propellant burning rate, vortex flow in the region of the nozzle could be used as a means for throttling a solid propellant rocket motor (ref. 58).

The larger motor size yielded a maximum pressure of 150 pounds per square inch absolute (1.05×10^6 N/sq cm). The same generators used in the smaller motor firings were used with the larger size. An initial exit diameter of 1.5 inches (3.81 cm) in the main chamber was found to yield a relatively low maximum pressure. This was reduced to 3/4-inch (1.91-cm) diameter by adapting a plug into the nozzle.

Instability in the motor with the 1/2-inch (1.27-cm) diameter nozzle persisted for a duration of 1/2 second sometime during the early portion of the firing whereas the 3/4-inch (1.91-cm) geometry oscillated throughout the entire firing. The mode of oscillation was the fundamental tengential mode as shown in figure 31. The tangential velocity was calculated from radial pressure measurements and the assumption of a free vortex. An instability region was mapped on a chamber pressure-tangential velocity plane (see fig. 32). This experimental instability behavior was matched to the response calculations described previously through the use of a velocity exponent of 0.6 in the burning rate expression (see fig. 33). It was only by inclusion of the velocity sensitive term that it was possible to match the calculations with the experimental data. The presence of the burning solid propellant in the main chamber is necessary in order to produce the mode of instability indicated in figure 31. That is, the propellant amplifies whatever small disturbances occur in the main chamber reaching very large amplitude. A test run without propellant in the main chamber showed no instability present. In this case the gas gen-

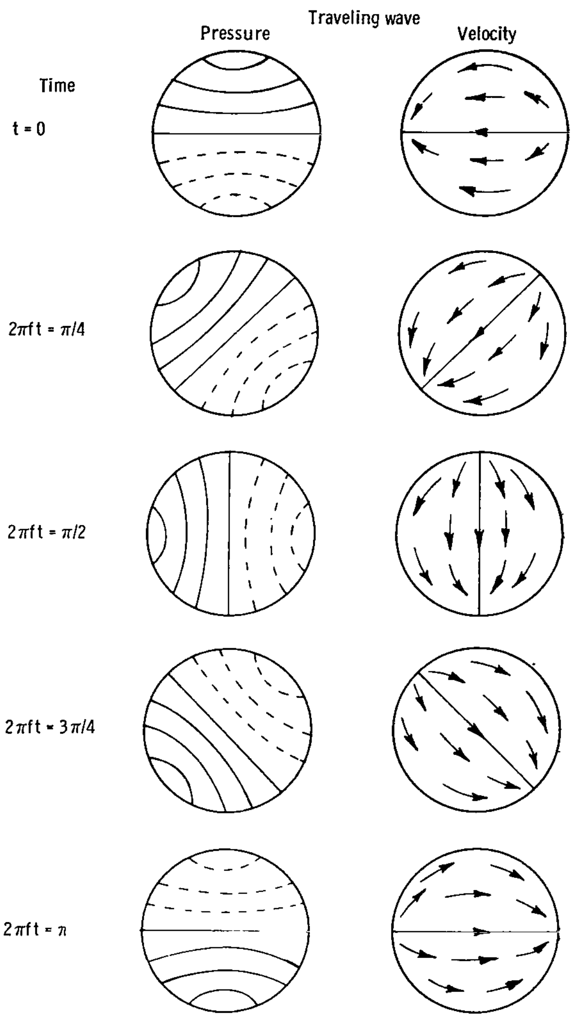

Figure 31. - Fundamental tangential mode of traveling waveform.

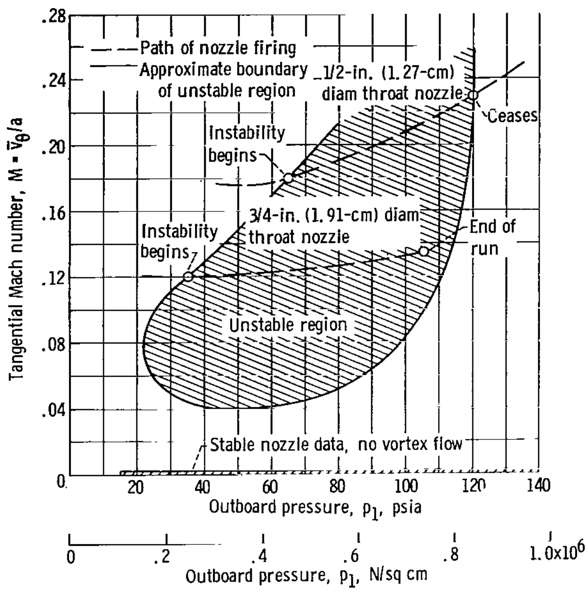

Figure 32. - Approximate region of unstable combustion (from ref. 14).

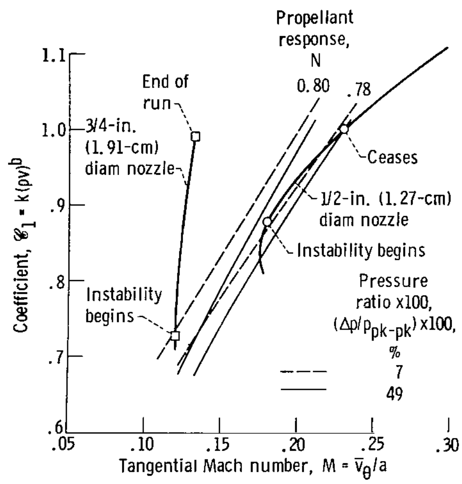

Figure 33. - Comparison of experimental burner data and calculated response curves. Combustion unstable to left of response curves (from ref. 14).

erator fed into the main chamber, which contained no propellant charge. Hence the phenomena being investigated are the direct result of an amplification of pressure disturbances by the burning propellant surface. Oscillation frequencies and amplitudes were measured for composite propellants. In the smaller motors the frequency was approximately 3800 cps decreasing with time. For the larger motor the frequency was 800 cps at the initiation of instability. Erosion patterns and flow fields within the combustor were also observed. The larger vortex motors used (24 in. (61.0 cm) diam.) had an $L/D \ll 1$.

The limited data obtained in these burners showed the fundamental traveling wave in the transverse direction can be sustained at frequencies around 800 cps.

The observations made in the vortex burner are similar to those observed in a conventional geometry (L/D > 1) by Swithenbank (refs. 10, 59, and 60). A single vortex was found to usually decrease the stability in the traveling tangential mode. Deliberate initiation of a standing mode by the use of two nitrogen T-jets, which reversed the tangential velocity four times around the periphery, was found to inhibit the formation of the traveling mode. This resulted in stable burning in an otherwise unstable configuration (ref. 59). In a rather ingeneous fashion, a herringbone thread was machined down the central conduit of the radial charge to produce the same effect as two T-jets. This scheme was also effective in producing stable operation in an otherwise highly unstable motor (ref. 59).

Aluminum and Al_2O_3 Effect

The addition of 1/2 percent by weight of fine aluminum powder (5 μm mean weight diam.) was found sufficient to damp out the high-frequency oscillation present in the com-

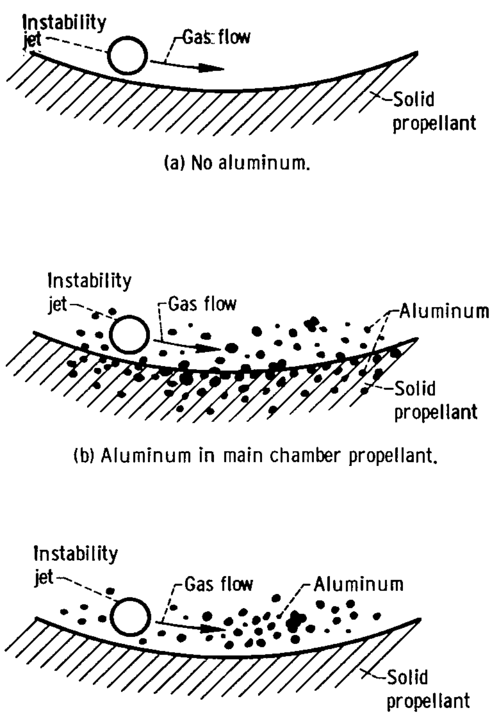

(a) No aluminum.

(b) Aluminum in main chamber propellant.

(c) Aluminum in generator propellant.

Figure 34. - Location of aluminum in propellant (from ref. 4).

bustor (ref. 4). Furthermore the inclusion of aluminum either in the main chamber or in the gas generator produced the same effect. The three situations tested are shown in figure 34 and the results in figures 35, 36, and 37. These results show that aluminum added in the gas phase was as effective in damping out transverse mode instability as the aluminum added as an original ingredient of the propellant. It was concluded that aluminum was effective in the gas phase in producing dissipative forces rather than producing a surface effect (ref. 4). It was further surmised that the mechanism of high-frequency damping is due to viscous and thermal effects (particulate damping). The validity of this conclusion was tested using an inert ingredient (Al_2O_3). Since some uncertainty exists regarding the particle size distribution resulting from the combustion of aluminized pro-

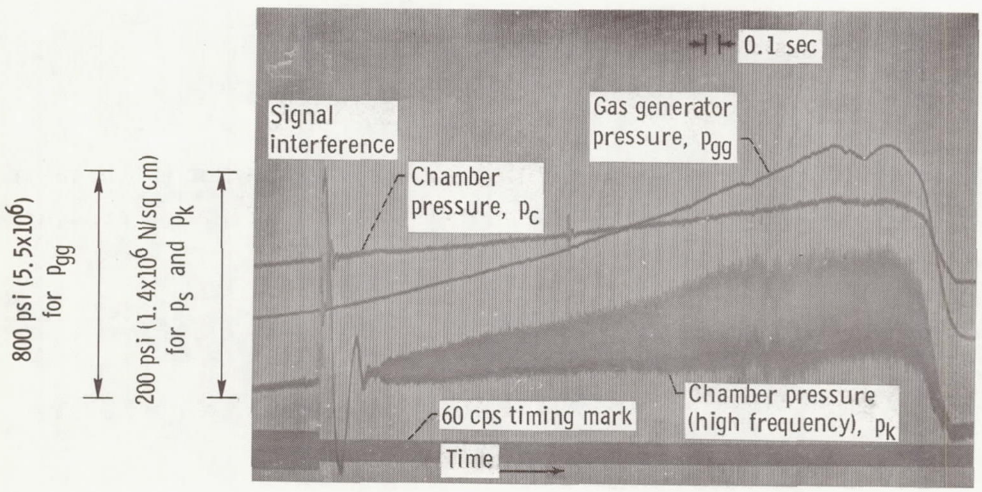

Figure 35. - Pressure-time trace without aluminum (from ref. 4).

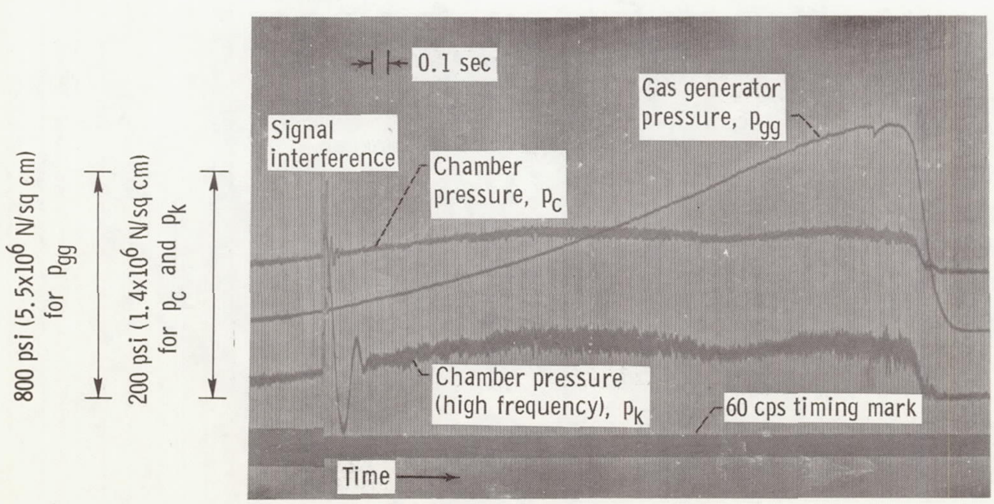

Figure 36. - Pressure-time trace with 1/2 percent aluminum in motor (from ref. 4).

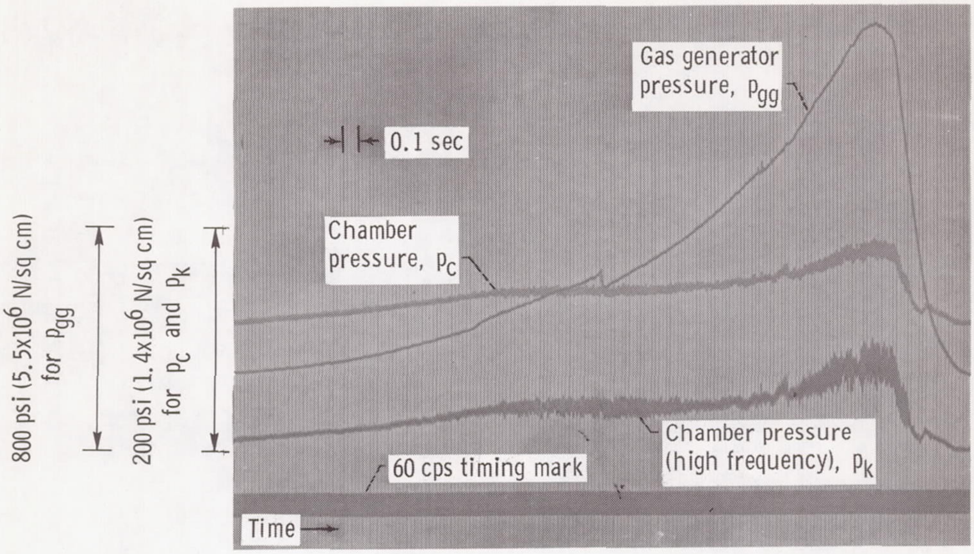

Figure 37. - Pressure-time trace with 1/2 percent aluminum in gas generator (from ref. 4).

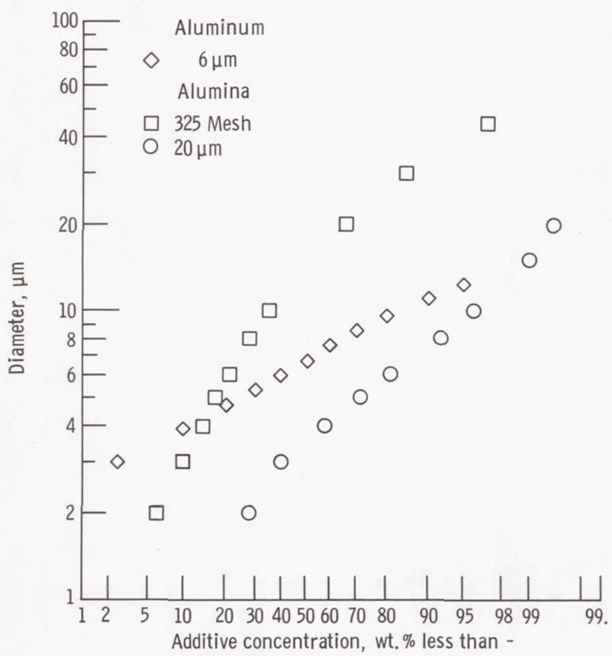

Figure 38. - Particle size distribution of metal additives as added to propellants.

pellant, two size ranges were used for the aluminum oxide as shown in figure 38. One range was generally finer than the initial aluminum distribution used and one was coarser. Comparison on a number basis between the Al_2O_3 (20 μm) and the burned aluminum size distribution as measured in a combustion environment (ref. 2) indicated fairly close size

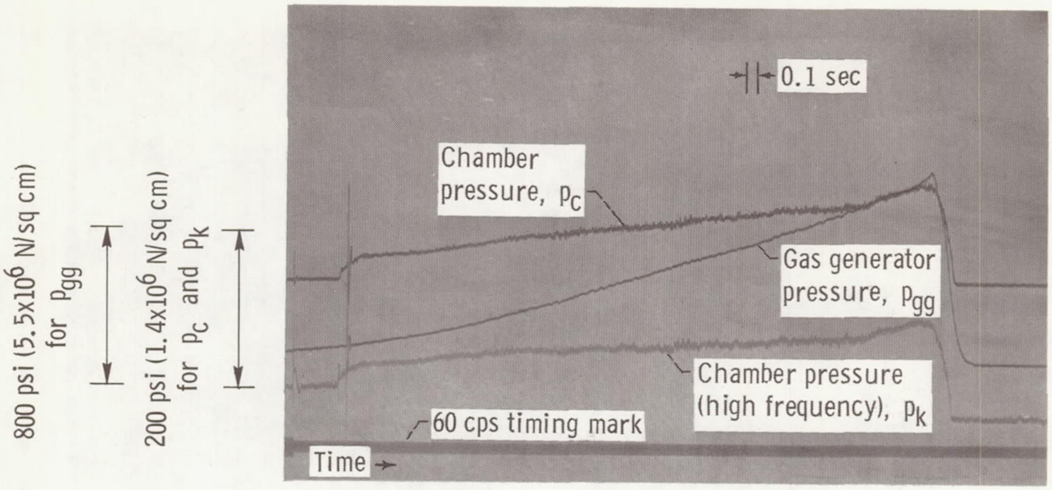

Figure 39. - Effect of Al_2O_3 on combustion instability: 1/2 percent by weight; throat diameter, 1/2 inch.

distributions. Tests with the 1/2 percent oxide of either size in the main chamber (fig. 39) indicated that the oxide does yield equivalent damping and supports the conclusion that the principal dissipative mechanism is particulate damping. In terms of affecting the analytical grain-loss balance for stability, the addition of Al or Al_2O_3 introduces particulate damping which raises the motor loss level. This loss level is determined by gas phase attenuation, viscoelastic losses, head end cavity losses, nozzle loss, and particulate damping. Referring to figure 40, raising the loss level to N_2 by additional damping means that the instability range is reduced to a $\overline{v}_\theta/a$ range of 2 to 3 rather than 1 to 4. Raising the loss level still higher to N_3 or greater means that no instability should occur. The additional loss due to particulate damping in the present work was believed to raise the loss level to the N_3 value or higher.

The acoustic attenuation was calculated using the mean value of the oxide particle size and the known concentration; the calculation is based on the particulate damping analysis of Epstein and Carhart (ref. 61). From reference 62 the attenuation is given by

$$\alpha = \frac{\overline{\alpha} C_m \omega}{a_o}$$

where $\overline{\alpha}$ is a dimensionless particulate acoustic attenuation. The dimensionless frequency $\omega\tau_D$ for the small vortex burner was calculated using

$$\omega\tau_D = \frac{\omega 2R^2\rho}{9\mu'} = 0.235$$

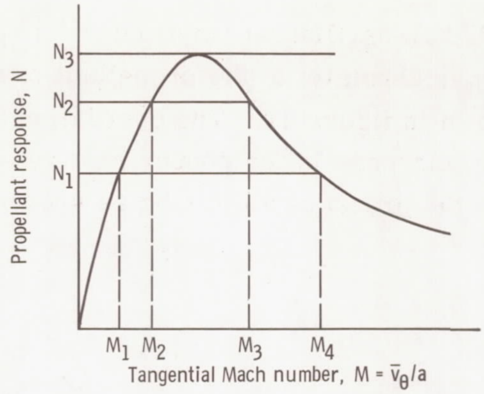

Figure 40. - Effect of propellant losses on instability range.

From figure 1 of reference 62, the corresponding values of $\overline{\alpha}$ for the present experiments is approximately 0.25. C_m is the mass concentration of particles, ω is the frequency, and a_o the sound velocity. Evaluation of the above expression gives a value of 0.2 foot^{-1} (0.66 m^{-1}) for α. Since the acoustic attenuation may be defined such that $\exp(-\alpha l)$ is the transmitted fraction of intensity after a disturbance traverses a distance l, αl $(I/I_o = e^{-\alpha l})$ was set equal to unity. Hence in the 5-inch (12.7-cm) diameter vortex burner, the pressure perturbation would decay to 1/e of its initial value in 4 cycles of oscillation. This calculation indicates that instability in the vortex burner, if initiated, would very quickly be damped out by the suspended Al or Al_2O_3 particles. The loss produced via the particulate damping is sufficient, therefore, to overcome the propellant gain or driving that is present.

Copper Chromite Effect

The reference propellant used in these experiments was a PBAA-ammonium per-

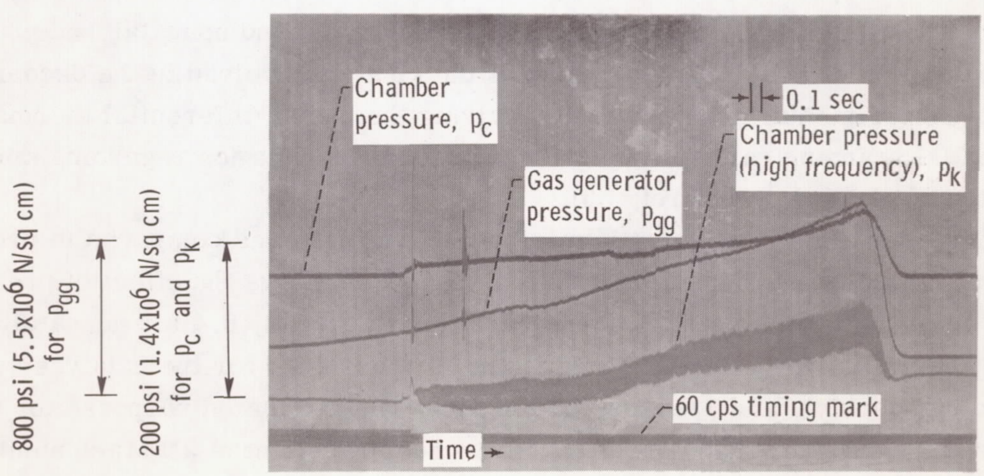

Figure 41. - Effect of 1/2 percent copper chromite on tangential mode instability.

chlorate mixture which yielded an oscillation amplitude of 55 percent. The addition of 1/2 percent by weight of copper chromite to the propellant caused the amplitude to increase to 85 percent, as shown in figure 41. The oscillation frequency remained the same as in the reference case. An increase in the copper chromite concentration to 3/4 percent caused a further rise in the pressure amplitude as shown in figure 42. The burning

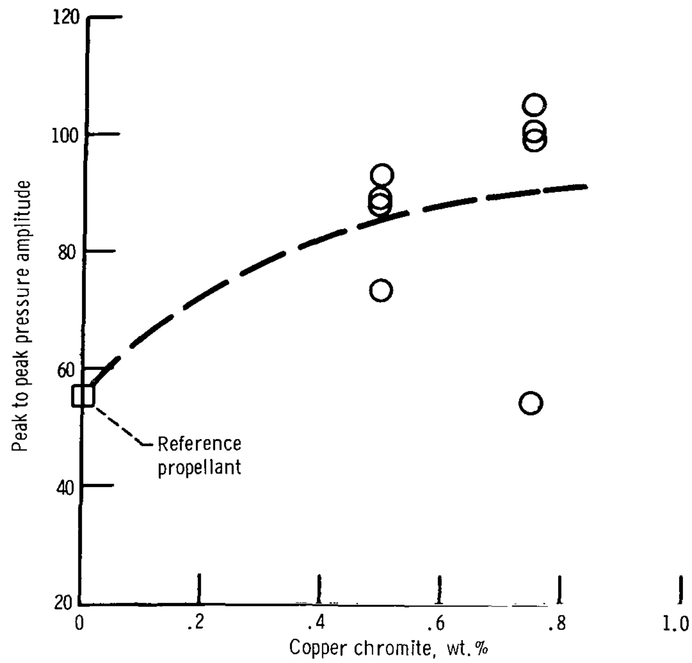

Figure 42. - Effect of copper chromite catalyst on amplitude of pressure oscillation.

rate change due to catalyst addition is shown in figure 43. It is noted that enhancement of the burning rate by the addition of higher percentages of ground oxidizer did not significantly affect the amplitude of the oscillations (ref. 14). Hence burning rate does not appear to be a sufficient criterion for comparing catalyzed and noncatalyzed propellants, suggesting the importance of consideration of the kinetics involved in the decomposition processes. Experimental investigations involving the use of differential thermal analysis and differential scanning calorimetry may yield some information regarding kinetic effects in the condensed phase (ref. 63).

The increased amplification with burning rate catalyst was compared to propellant response calculations mentioned previously. Figure 44 shows the effect of pressure exponent n, as measured in a strand burner (0.6 for catalyzed, 0.4 for noncatalyzed), the erosive exponent (0.6 for reference propellant, 0.5 assumed for the catalyzed propellant), $\mathscr{C}_1$ (defined previously), and pressure amplitude. The calculated response for the catalyzed propellant is higher than that of the reference propellant at all Mach numbers, indicating a greater tendency toward instability. Qualitatively, this is an agreement with the experimental results. Higher amplitude response was not calculated due to the approxi-

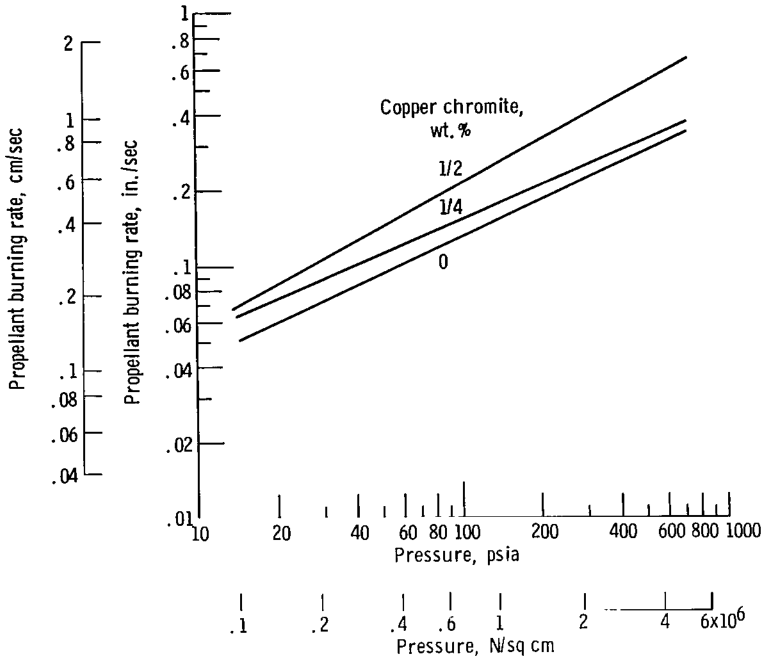

Figure 43. - Effect of burning rate catalyst on PBAA (19 percent) - AP (81 percent) propellant.

mations in the theory and in the values of $\mathscr{C}_1$ and the erosive exponent m for the catalyzed propellant.

The increased amplification observed is not in agreement with published T-burner results at the same frequency (ref. 64). Figure 45 shows the propellant response as a function of frequency for fine oxidizer propellant and fine oxidizer plus 1 percent copper

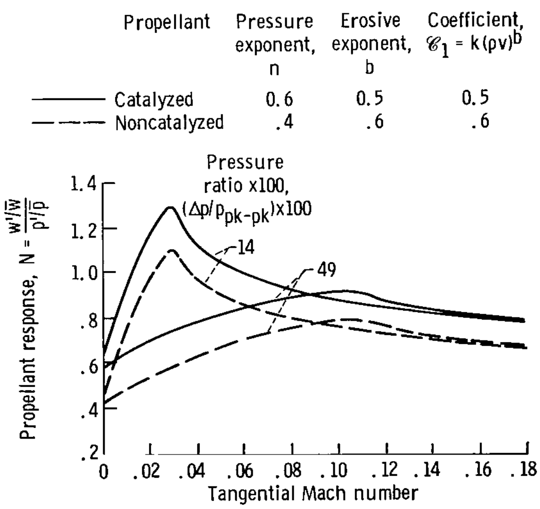

Figure 44. - Theoretical propellant pressure and velocity response.

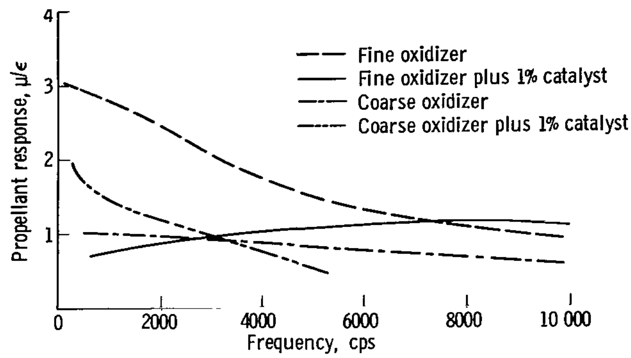

Figure 45. - Effect of copper chromite catalyst on experimental response functions from T-burner (from ref. 64).

chromite and similar curves for coarse oxidizer propellants. At 3000 to 4000 cps the fine oxidizer curve is significantly larger than the fine oxidizer plus 1 percent curve, indicating that more driving (greater instability) is present in the uncatalyzed propellant. For the coarse oxidizer propellant the response is of comparable value for the catalyzed and noncatalyzed propellants. Hence, the T-burner results do not yield general agreement with the vortex burner results. The propellants used in the vortex were predominately coarse oxidizer propellants which could account for some of the variation. However, it is believed that the principal cause of the difference in the results is due to the fact that the T-burner measures only a pressure response whereas the vortex burner incorporates both pressure and velocity coupling effects.

RELEVANCE TO ROCKET MOTORS

In regard to the experimental work performed in the vortex burner, the question arises as to whether or not high mean velocities occur in rocket motors. It is noted, first, that erosion may occur with some propellant compositions at low flow velocities. Therefore, it is the amount of erosive burning rather than the magnitude of the velocity that is important. In the vortex burner experiment it was calculated that the tangential flow caused less than 10 percent erosion. This small amount of erosion was the determining factor in establishing the response curves. Secondly, it is noted that evidence of tangential flow in full scale motors does indeed exist. For instance the Scout ST-1 third stage is believed to have oscillated in the tangential mode accompanied by a roll disturbance. This disturbance appears to result from a nonlinear viscous phenomena (acoustic streaming) which occurs in the presence of large amplitude wave motion (ref. 65). Highly unstable motors with cylindrical grain performations are especially subject to roll torque generation, although similar effects are exhibited in other complex grain configurations such as star perforated cavities. The presence of vortices have been observed at

TABLE I. - IMPORTANT PARAMETERS REQUIRED FOR STABILITY DETERMINATION[a]

[From ref. 70.]

Quanity	Mechanism	Function of -
Admittance of burning layer	Causes amplification or attenuation at the burning surface	Frequency, pressure propellant temperature, erosive velocity
Gas-phase damping length or attenuation coefficient	Causes amplification or attenuation in the gas phase	Propellant composition, curing time, method of cure, etc.
Solid-phase viscoelastic constants	Contributes to determining mode frequencies and to attenuation in the solid phase	Frequency, pressure, propellant temperature
Nozzle admittance	Contributes to determining mode frequencies and to gain or loss at the nozzle plane	Frequency, mode, mean flow distribution, nozzle size and shape, sound velocity in gas, and the sound field itself

[a]Other parameters as well, such as those describing wall losses, resonant rod losses, inputs due to aerodynamic screaming, etc. may occasionally be important.

Sheffield University and Summerfield Station through head end windows on rocket motors. Furthermore, values of the tangential velocity of the order of 400 feet per second (122 m/sec) of the acoustic streaming vortex, whether initiated by injected gases or by spontaneous instability, have been measured in rocket motors (ref. 56). Spin-stabilized rocket stages may also give rise to tangential flow. It appears, therefore, that there is a strong possibility of tangential flow in rocket motors coupled with transverse acoustic modes. The nature of these modes and the accompanying fluid motion make it necessary to investigate velocity effects as well as those of pressure.

The accuracy with which motor stability can be predicted will remain dependent on the ability to determine individual gains and losses in a particular motor design. The suppressive mechanisms include viscous wall effects, bulk viscosity, head end cavity reflections, mixing losses, convective and radiative energy losses through the nozzle, viscoelastic attenuation, and particulate damping (refs. 31 and 53). The complexity of the required understanding is illustrated in table I.

Dynamic testing of motor systems as a requirement for stability may also be required, particularly if large solid boosters are used for manned systems. Only when the results of this highly interdisciplinary research yield the relative values of the driving-damping factors (refs. 66 to 69) will the gap that separates propellant research and motor design be eventually bridged.

CONCLUSIONS

In order to successfully calculate propellant amplification it is necessary to employ modeling techniques which embody the essential ingredients of the burning process under dynamic conditions. Evidence exists that several additional factors need to be considered in order to obtain agreement between theory and experiment. These factors are concerned with the (a) reaction zone structure and (b) velocity sensitivity:

1. The flame zone structure is not sufficiently well understood presently. Some recent evidence, discussed in this report, indicates that flame thickness may be appreciable in magnitude. This concept of a distributed or thick reaction zone necessitates the inclusion of time-dependent mixing terms in the analytical formulation of response models. In addition, the description of the burning process in quasi-steady form is nonrealistic at high frequencies and the use of an Arrhenius expression is deficient in that it does not consider the realities of the inhomogeniety of composite propellants. The contribution of exothermic surface reactions also appears to be an important requirement.

2. The calculated response factors presented in this report for the vortex burner (i.e., figs. 25 and 26) are dependent on both the velocity and pressure sensitivity of the propellant burning process. Based on the wave amplification mechanism assumed (illustrated in fig. 24), the velocity sensitivity exerted the predominant influence on the response curve shape, whereas pressure serves only to change the response magnitude by a fixed amount independent of velocity. Hence it is the sensitivity to velocity that exerts the predominant influence on the occurrence and cessation of instability. Propellant erosion is recognized therefore to play a dominant role in stability behavior. Similar results were obtained in the nonlinear calculations presented in reference 54, where erosion was found to exert a drastic change on the stability boundaries (i.e., fig. 17). The addition of velocity sensitivity, through erosion, served to increase amplification or propellant driving. In both of these previous works, the addition of velocity sensitivity served to increase the gain. It is concluded, therefore, that combined pressure and velocity sensitivity lead to a less stable system than does pressure sensitivity alone. Hence rating techniques which neglect velocity coupling may yield misleading results relative to the occurrence of transverse mode combustion instability.

It is precisely these combined pressure-velocity effects that can be studied with the aid of the vortex burner or modified T-burner. These small-scale research burners should be capable of determining further contributions of the combined pressure-velocity fields to the measurement of the propellant response under conditions which more realistically approach an actual rocket combustion environment. This information will eventually culminate in a more thorough understanding of the instability phenomena and lead to the "a priori design" of stable rocket motors. This will be accomplished by providing critical data required for the verification or modification of prevalent theoretical work aimed at providing response data. The improved response data would then be coupled with a more exact determination of the losses in a given system to determine the amplification-attenuation balance.

Lewis Research Center,
National Aeronautics and Space Administration,
Cleveland, Ohio, May 26, 1969,
722-03-00-06-22.

REFERENCES

1. Watermeier, L. A.; Aungst, W. P.; Pfaff, S. P.: An Experimental Study of the Aluminum Additive Role in Unstable Combustion of Solid Rocket Propellants. Ninth Symposium (International) on Combustion, Academic Press, 1963, pp. 316-327.
2. Povinelli, Louis A.; and Rosenstein, Robert A.: Alumina Size Distributions from High-Pressure Composite Solid-Propellant Combustion. AIAA J., vol. 2, no. 10, Oct. 1964, pp. 1754-1760.
3. Crump, J. E.: Aluminum Combustion in Composite Propellatns. 2nd ICRPG Combustion Conference. Vol. I. Rep. CPIA Publ.-105, Applied Physics Lab., Johns Hopkins Univ., May 1966, pp. 321-329. (Available from DDC as AD-484561.)
4. Povinelli, Louis A.: Particulate Damping in Solid-Propellant Combustion Instability. AIAA J., vol. 5, no. 10, Oct. 1967, pp. 1791-1796.
5. Coates, R. L.: Research on Combustion of Solid Propellants. LPC-641-F, Lockheed Propulsion Co., Dec. 30, 1965. (Available from DDC as AD-482863.)
6. Dickinson, L. A.: Command Initiation of Finite Wave Axial Combustion Instability in Solid Propellant Rocket Engines. ARS J., vol. 32, no. 4, Apr. 1962, pp. 643-644.
7. Dickinson, L. A.; and Jackson, F.: Combustion in Solid Propellant Rocket Engines. Combustion and Propulsion; Fifth AGARD Colloquium. Macmillan Co., 1963, pp. 531-544.
8. Morris, E. P.: A Pulse Technique For the Evaluation of Combustion Instability in Solid Propellant Rocket Motors. Can. Aeron. Space J., vol. 11, no. 9, Nov. 1965, pp. 329-333.
9. Povinelli, Louis A.: Velocity Sensitivity in Transverse Mode Solid Propellant Combustion Instability. 3rd ICRPG Combustion Conference. Vol. 1. Rep. CPIA-Publ.-138, Applied Physics Lab., Johns Hopkins Univ., Feb. 1967, pp. 255-258. (Available from DDC as AD-807276.)

10. Swithenbank, J.; and Sotter, G.: Vortex Generation in Solid Propellant Rockets. AIAA J., vol. 2, no. 7, July 1964, pp. 1297-1302.

11. Price, E. W.; and Dehority, G. L.: Velocity Coupled Axial Mode Combustion Instability in Solid Propellant Rocket Motors. 3rd ICRPG Combustion Conference. Vol. 1. Rep. CPIA-Publ.-138, Applied Physics Lab., Johns Hopkins Univ., Feb. 1967, pp. 313-319. (Available from DDC as AD-807276.)

12. Stepp, E. E.: Effect of Pressure and Velocity Coupling on Low-Frequency Instability. AIAA J., vol. 5, no. 5, May 1967, pp. 945-948.

13. Price, E. W.: Evidence for Velocity-Coupling. 1st ICRPG Combustion Conference. Vol. 1. Rep. CPIA-68, Applied Physics Lab., Johns Hopkins Univ., Jan. 1965, pp. 403-408. (Available from DDC as AD-458060.)

14. Povinelli, Louis A.; Heidmann, Marcus F.; and Feiler, Charles E.: Experimental Investigation of Transverse-Mode Solid-Propellant Combustion Instability in a Vortex Burner. NASA TN D-3708, 1966.

15. Trubridge, G. F. P.: Unstable Burning in Solid Propellant Rocket Motors. J. Brit. Interplanetary Soc., vol. 20, pt. 2, Apr. 1965, pp. 33-42.

16. Hart, R. W.; and McClure, F. T.: Theory of Acoustic Instability in Solid-Propellant Rocket Combustion. Tenth Symposium (International) on Combustion. The Combustion Institute, 1965, pp. 1047-1065.

17. Price, E. W.: Experimental Solid Rocket Combustion Instability. Tenth Symposium (International) on Combustion. The Combustion Institute, 1965, pp. 1067-1082.

18. Price, E. W.: Status of Solid Rocket Combustion Instability Research Rep. NOTS-TP-4275, Naval Ordnance Test Station, Feb. 1967. (Available from DDC as AD-650200.)

19. Schultz, R.; Green, L.; and Penner, S. S.: Studies of the Decomposition Mechanism, Erosion Burning and Resonance for Solid Composite Propellants. Combustion and Propulsion; Third AGARD Colloquium. Pergamon Press, 1958, pp. 367-427.

20. McClure, F. T.; Hart, R. W.; and Bird, J. F.: Solid Propellant Rocket Motors as Acoustic Oscillators. Progress in Astronautics and Rocketry. Vol. 1. Academic Press, 1960, pp. 295-358.

21. Ryan, N. W.; Coates, R. L.; and Baer, A. D.: Participation of the Solid Phase in the Oscillatory Burning of Solid Rocket Propellants. Ninth Symposium (International) on Combustion. Academic Press, 1963, pp. 328-332.

22. Angelus, T. A.: Unstable Burning Phenomenon in Double-Base Propellants. Progress in Astronautics and Rocketry. Vol. 1. Academic Press, 1960, pp. 527-559.

23. Horton, M. D.; and Price, E. W.: Dynamic Characteristics of Solid Propellant Combustion. Ninth Symposium (International) on Combustion. Academic Press, 1963, pp. 303-310.

24. Cantrell, R. H.; McClure, F. T.; and Hart, R. W.: Effects of Thermal Radiation on the Acoustic Response of Solid Propellants. AIAA J., vol. 3, no. 3, Mar. 1965, pp. 418-426.

25. Culick, F. E. C.: A Review of Calculations of the Admittance Function for a Burning Surface. App. A. Combustion of Solid Propellants and Low Frequency Combustion Instability. Rep. NOTS-TP-4244, Naval Ordnance Test Station (NASA CR-97175), June 1967. (Available from DDC as AD-832496.)

26. Bird, J. F.; Hart, R. W.; and McClure, F. T.: Finite Acoustic Oscillations and Erosive Burning in Solid Fuel Rockets. AIAA J., vol. 3, no. 12, Dec. 1965, pp. 2248-2256.

27. Hart. R. W.; Farrell, R. A.; and Cantrell, R. H.: Theoretical Study of a Solid Propellant Having a Heterogeneous Surface Reaction. I - Acoustic Response, Low and Intermediate Frequencies. Combustion and Flame, vol. 10, Dec. 1966, pp. 367-380.

28. Denison, M. Richard; and Baum, Eric: A Simplified Model of Unstable Burning in Solid Propellants. ARS J., vol. 31, no. 8, Aug. 1961, pp. 1112-1122.

29. Capener, E. L., et al.: Response of a Burning Propellant Surface to Erosive Transients. Stanford Research Inst. (AFOSR-67-0859, DDC No. AD-810778), Dec. 1966.

30. Culick, F. E. C.: Calculation of the Admittance Function for a Burning Surface. Astronautica Acta, vol. 13, no. 3, May-June 1967, pp. 221-237.

31. Marxman, G. A.; and Wooldridge, C. E.: Effect of Surface Reactions on the Solid Propellant Response Function. AIAA J., vol. 6, no. 3, Mar. 1968, pp. 471-478.

32. Brown, R. S.; Muzzy, R. J.; and Steinle, M. E.: Surface Reaction Effects on the Acoustic Response of Composite Solid Propellants. AIAA J., vol. 6, no. 3, Mar. 1968, pp. 479-488.

33. Friedly, John C.; and Petersen, Eugene E.: Influence of Combustion Parameters on Instability in Solid Propellant Motors: Part I. Development of Model and Linear Analysis. AIAA J., vol. 4, no. 9, Sept. 1966, pp. 1604-1610.

34. Beckstead, M. W.: Low Frequency Instability - A Comparison of Theory and Experiment. Paper 67-13, Western States Section, Combustion Institute, Apr. 1967.

35. Culick, F. E. C.: A Review of Calculations for Unsteady Burning of a Solid Propellant. AIAA J., vol. 6, no. 12, Dec. 1968, pp. 2241-2255.

36. Beckstead, Merrill W.; and Culick, F. E. C.: A Comparison of Analysis and Experiment for the Response Function of a Burning Surface. 4th ICRPG Combustion Conference. Vol. 1. Rep. CPIA-Publ.-162, Applied Physics Lab., Johns Hopkins Univ., Dec. 1967, pp. 331-336. (Available from DDC as AD-828010.)

37. Horton, M. D.: Reply to Discussion on Dynamic Characteristics of Solid Propellant Combustion by M. D. Horton and E. W. Price. Ninth Symposium (International) on Combustion, Academic Press, 1963, p. 333.

38. Krier, H.; Tien, J. S.; Sirignano, W. A.; and Summerfield, M.: Non-Steady Burning Phenomena of Solid Propellants: Theory and Experiments. ICRPG/AIAA 2nd Solid Propulsion Conference. AIAA, 1967, pp. 75-88.

39. Williams, F. A.: Theoretical Considerations Concerning Models for Effect of Solid Heterogeneity on Oscillatory Combustion. Presented at the ICRPG/AIAA 3rd Solid Propulsion Conference, 1968.

40. Povinelli, Louis A.: Some Aspects of Steady-State Propellant Combustion as Related to Dynamic Coupling Mechanisms. Presented at Conference on Mechanisms of Coupling of Combustion with Gas Dynamic Flow Fields, Princeton University, Jan. 25-26, 1968.

41. Povinelli, Louis A.: Spectrographic Measurements of Composite Propellant Flame Zone Structure. 1st ICRPG Combustion Conference. Vol. 1. Rep. CPIA-68, Applied Physics Lab., Johns Hopkins Univ., Jan. 1965, pp. 331-333. (Available from DDC as AD-458060.)

42. Povinelli, Louis A.: A Study of Composite Solid-Propellant Flame Structure Using a Spectral Radiation Shadowgraph Technique. AIAA J., vol. 3, no. 9, Sept. 1965, pp. 1593-1598.

43. Waesche, R. H. Woodward: The Effects of Pressure and Formulation on the Emission Spectra of Solid Propellants. 3rd ICRPG Combustion Conference. Vol. 1. Rep. CPIA-Publ.-138, Applied Physics Lab., Johns Hopkins Univ., Feb. 1968, p. 123. (Avaialble from DDC as AD-807276.)

44. Derr, R. L.; and Osborn, J. R.: An Experimental Investigation of the Gaseous Phase Reaction Zone in a Composite Solid Propellant. Rep. TM-67-6, JPC-438, Jet Propulsion Center, Purdue University (NASA CR-90226), Sept. 1967.

45. Penzias, Gunter J.; Liang, Eliot T.; and Tourin, Richard H.: Infrared Radiation and Temperature Measurements in Solid Propellant Flames. I. Preliminary Study of ARCITE 368. Rep. TR 800-5, Warner and Swasey Co., Oct. 1962.

46. Summerfield, M., et al.: Burning Mechanisms of Ammonium Perchlorate Propellants. Progress in Astronautics and Rocketry. Vol. 1. Academic Press, 1960, pp. 141-182.

47. Friedman, Raymond: Experimental Techniques for Solid-Propellant Combustion Research. AIAA J., vol. 5, no. 7, July 1967, pp. 1217-1223.

48. Sabadell, A. J.; Wenograd, J.; and Summerfield, M.: Measurement of Temperature Profiles Through Solid-Propellant Flames Using Fine Thermocouples. AIAA J., vol. 3, no. 9, Sept. 1965, pp. 1580-1584.

49. Anderson, Ralph; Brown, Robert S.; and Shannon, Larry J.: Heterogeneous Reactions in Ignition and Combustion of Solid Propellants. AIAA J., vol. 2, no. 1, Jan. 1964, pp. 179-180.

50. Hightower, J. D.; and Price, E. W.: Two-Dimensional Experimental Studies of the Combustion Zone of Composite Propellants. Presented at the 2nd ICRPG Second Combustion Conference, Oct. 1965.

51. McGurk, J. L.: Microscopic Determination of Propellant Combustion Surface Temperatures. 1st ICRPG Combustion Conference. Vol. 1. Rep. CPIA-68, Applied Physics Lab., Johns Hopkins Univ., Jan. 1965, pp. 345-359. (Available from DDC as AD-458060.)

52. Hightower, J. D.; and Price, E. W.: Combustion of Ammonium Perchlorate. Eleventh Symposium (International) on Combustion. The Combustion Institute, 1967, pp. 463-472.

53. Friedly, John C.; and Petersen, Eugene E.: Influence of Combustion Parameters on Instability in Solid Propellant Motors. Part II: Nonlinear Analysis. AIAA J., vol. 4, no. 11, Nov. 1966, pp. 1932-1937.

54. Povinelli, Louis A.: One-Dimensional Nonlinear Model for Determining Combustion Instability in Solid Propellant Rocket Motors. NASA TN D-3410, 1966.

55. Price, E. W.; Rice, D. W.; and Crump, J. E.: Low-Frequency Combustion Instability of Solid Rocket Propellants. Rep. NOTS-TP-3524, Naval Ordnance Test Station, July 1964. (Available from DDC as AD-443438.)

56. Swithenbank, J.; Stones, J. L.; and Willis, J. D.: Investigation of Unstable Combustion in Solid Propellant Rockets. 3rd ICRPG Combustion Conference. Vol. 1. Rep. CPIA-Publ.-138, Applied Physics Lab., Johns Hopkins Univ., Feb. 1967, p. 277. (Available from DDC as AD-807276.)

57. Maslen, Stephen H.; and Moore, Franklin K.: On Strong Transverse Waves Without Shocks in a Circular Cylinder. J. Aeron. Sci., vol. 23, no. 6, June 1956, pp. 583-593.

58. Povinelli, Louis A.; and Heidmann, Marcus F.: Burning Rate Control for Solid Propellants. U.S. Patent 3,345,822, 1966.

59. Swithenbank, J.: Non-Linear Behavior of Solid Propellant Rocket Combustion Instability. 2nd ICRPG Combustion Conference. Vol. I. Rep. CPIA-Publ.-105, Applied Physics Lab., Johns Hopkins Univ., May 1966, pp. 719-760. (Available from DDC as AD-484561.)

60. Swithenbank, J.; and Sotter, J. G.: Vorticity in Solid Propellant Rocket Motors. 14th International Aeronautical Congress. Vol. 1. Gauthier-Villars, Paris, 1965, pp. 249-275.

61. Epstein, Paul S.; and Carhart, Richard R.: The Absorption of Sound in Suspensions and Emulsions. I. Water Fog in Air. J. Acoust. Soc. Am., vol. 25, no. 3, May 1953, pp. 553-565.

62. Dobbins, Richard A.; and Temkin, Samuel: Propagation of Sound in a Gas-Particle Mixture and Acoustic Combustion Instability. AIAA J., vol. 5, no. 12, Dec. 1967, pp. 2182-2186.

63. Wenograd, J.: Study of the Kinetics and Energetics of Propellant Decomposition Reactions and Application to Steady-State Combustion Mechanism. 3rd ICRPG Combustion Conference. Vol. 1. Rep. CPIA-Publ.-138, Applied Physics Lab., Johns Hopkins Univ., Feb. 1967, pp. 89-94. (Available from DDC as AD-807276.)

64. Horton, M. D.; and Rice, D. W.: The Effects of Compositional Variables Upon Oscillatory Combustion of Solid Rocket Propellants. Combustion and Flame, vol. 8, no. 1, Mar. 1964, pp. 21-28.

65. Flandro, G. A.: Roll Torque and Normal Force Generation in Acoustically Unstable Rocket Motors. AIAA J., vol. 2, no. 7, July 1964, pp. 1303-1306.

66. McClure, F. T.; Hart, R. W.; and Cantrell, R. H.: Interaction Between Sound and Flow: Stability of T-Burners. AIAA J., vol. 1, no. 3, Mar. 1963, pp. 586-590.

67. Hart, R. W.; and Cantrell, R. H.: Amplification and Attenuation of Sound by Burning Propellants. AIAA J., vol. 1. no. 2, Feb. 1963, pp. 398-404.

68. Cantrell, R. H.; and Trubridge, G. F. P.: A Program for Pre-Firing Prediction of High Frequency Combustion Instability in Solid Propellant Rocket Motors. 2nd ICRPG Combustion Conference. Vol. I. Rep. CPIA-Publ.-105, Applied Physics Lab., Johns Hopkins Univ., May 1966, pp. 617-640. (Available from DDC as AD-484561.)

69. Jenks, J. C.: An Experimental Program for the Prefiring Prediction of Acoustic Instability in Solid Propellant Rocket Motors. 4th ICRPG Combustion Conference. Vol. 1. Rep. CPIA-Publ.-162, Applied Physics Lab., Johns Hopkins Univ., Dec. 1967, pp. 353-360. (Available from DDC as AD-828010.)

70. Hart, R. W.; and Bird, J. F.: Scaling Problems Associated with Unstable Burning in Solid Propellant Rockets. Ninth Symposium (International) on Combustion. Academic Press, 1963, pp. 993-1004.

NASA-Langley, 1969 —— 33 E-4574

NATIONAL AERONAUTICS AND SPACE ADMINISTRATION
WASHINGTON, D. C. 20546

OFFICIAL BUSINESS

FIRST CLASS MAIL

POSTAGE AND FEES PAID
NATIONAL AERONAUTICS AND
SPACE ADMINISTRATION

POSTMASTER: If Undeliverable (Section 158 Postal Manual) Do Not Return

"The aeronautical and space activities of the United States shall be conducted so as to contribute . . . to the expansion of human knowledge of phenomena in the atmosphere and space. The Administration shall provide for the widest practicable and appropriate dissemination of information concerning its activities and the results thereof."

— NATIONAL AERONAUTICS AND SPACE ACT OF 1958

NASA SCIENTIFIC AND TECHNICAL PUBLICATIONS

TECHNICAL REPORTS: Scientific and technical information considered important, complete, and a lasting contribution to existing knowledge.

TECHNICAL NOTES: Information less broad in scope but nevertheless of importance as a contribution to existing knowledge.

TECHNICAL MEMORANDUMS: Information receiving limited distribution because of preliminary data, security classification, or other reasons.

CONTRACTOR REPORTS: Scientific and technical information generated under a NASA contract or grant and considered an important contribution to existing knowledge.

TECHNICAL TRANSLATIONS: Information published in a foreign language considered to merit NASA distribution in English.

SPECIAL PUBLICATIONS: Information derived from or of value to NASA activities. Publications include conference proceedings, monographs, data compilations, handbooks, sourcebooks, and special bibliographies.

TECHNOLOGY UTILIZATION PUBLICATIONS: Information on technology used by NASA that may be of particular interest in commercial and other non-aerospace applications. Publications include Tech Briefs, Technology Utilization Reports and Notes, and Technology Surveys.

Details on the availability of these publications may be obtained from:

SCIENTIFIC AND TECHNICAL INFORMATION DIVISION

NATIONAL AERONAUTICS AND SPACE ADMINISTRATION

Washington, D.C. 20546